Synthesizing and Evaluating Photodynamic Efficacy of Asymmetric Heteroleptic Novel A_7B Type Bis-Lanthanide(III) Phthalocyanine Complexes

Emel Önal[a,b], Özge Tüncel[c] , Mohamad Albakour[a], Gizem Gümüşgöz Çelik[a], Ayşe Gül Gürek[a*], Serdar Özçelik[c*]

[a] *Gebze Technical University, Department of Chemistry, Gebze, 41400 Kocaeli, Turkey*

[b] *Doğuş University, Faculty of Engineering, Ümraniye, 34775 Istanbul, Turkey*

[c] *Izmir Institute of Technology, Faculty of Science, Department of Chemistry, Urla, 35430 Izmir, Turkey*

Supporting Information

Table of Contents………………………………………………………………………………. Page

1. General Information

Reagents and solvents: All reagents, purchased from fine chemical suppliers Aldrich, Merck, Alfa Aesar, and Fluka, were used without further purification unless otherwise stated. Solvents were either used as commercially supplied or used as purified by standard techniques.

Methods : Nonaqueous reactions were performed in oven-dried glassware under argon atmosphere at reported temperature. Reactions were monitored by thin layer chromatography on Merck silica gel 60 F254 precoated aluminum sheets. Spots were visualized either by UV 254 nm light. Column chromatography was performed on Merck silica gel 60 (230-400 mesh size) or preparative TLC (silica gel) using the appropriate solvent system as eluent.

Infrared Spectroscopy : Infrared spectra were recorded on a PerkinElmer Spectrum 100 FT-IR spectrometer with an attenuated total reflection (ATR) accessory featuring diamond/ZnSe plate. Samples were deposited as neat on ATR module and absorption maxima (ν_{max}) were quoted in wavenumbers (cm^{-1}) in the range of 4000-650 cm^{-1}. Intensities of absorptions are abbreviated as s, strong; m, medium; and w, weak.

NMR Spectroscopy : ^1H and ^{13}C nuclear magnetic resonance spectra were taken on Bruker Ultrashield Plus 400 MHz FT-NMR spectrometer. Deuterated solvents were used in all NMR measurements. Chemical shifts (δ) are reported in parts per million (ppm) relative to residual solvent peaks as an internal reference for ^1H-^{13}C nuclei. Assignments were determined on the basis of either unambiguous chemical shift or coupling patterns. Peak multiplicities are defined as s = singlet, d = doublet, t = triplet, q = quartet, m = multiplet, br = broad.

Mass Spectra : Matrix-assisted laser desorption ionization time-of-flight (MALDI-TOF) mass spectra were recorded on a BRUKER Microflex LT spectrometer. The matrix is indicated in brackets for each compound.

Absorption Spectroscopy : Absorption spectra were recorded at room temperature on a Shimadzu UV-2600 UV-vis and UV-VIR spectrometer using a 1 cm path length quartz cuvette between maximum range 300 and 1400 nm. Solutions were prepared in spectro-grade solvents. Molar extinction coefficients (ε) were determined by measurement of the absorption of t five solutions of differing concentration for each radical, followed by determination of the slope.

Photophysical and Photochemical Measurements: Steady-state fluorescence excitation and emission spectra were recorded by using a Varian Cary Eclipse spectrofluorometer using 10 mm path length cuvettes at room temperature. ***Fluorescence quantum yield (ϕ_F) determination.*** Fluorescence quantum yield values (ϕ_F) were determined by using William's method [1]. Accordingly, the UV-Vis absorbance and fluorescence emission spectra at different concentrations of the reference standard (**ZnPc**) and samples were measured under identical conditions. Integrated fluorescence intensities versus absorbance for **ZnPc** (ϕ_F= 0.18 in DMSO [2]) and **LnPcs** were plotted. Slopes of the plots were proportional to the quantity of the quantum yield. Equation 1 was used to calculate quantum yield (ϕ_F) values. In the equation, Grad is the gradient of the plot and n is the refractive index of the solvent used for samples and standards.

$$\Phi_F = \Phi_F^{Std}\left(\frac{Grad}{Grad_{Std}}\right)\left(\frac{n^2}{n_{Std}^2}\right) \qquad (1)$$

Singlet oxygen quantum yield (Φ_Δ) determination. For indirect method, singlet oxygen quantum yield (Φ_Δ) determinations were carried out a 1 mL portion of the solutions containing the singlet oxygen quencher irradiated in the Q band region with the photo-irradiation set-up described in the reference [3]. For singlet oxygen measurements, DPBF was used as chemical quencher (Φ_Δ **ZnPc** = 0.67 in DMSO [4]). DPBF degradation at 417 nm was monitored by UV-Vis spectroscopy. The solutions of 1×10^{-5} M of **LnPc** complexes (2.5 mL) containing DPBF 1 mL (~1×10^{-5} M) were prepared in the dark and irradiated in the Q band region. The light intensity of 7.05×10^{15} photons s^{-1} cm^{-2} was used for Φ_Δ determinations. Singlet oxygen quantum yields (Φ_Δ) were calculated using the equation 2. In the equation, R and R_{Std} were DPBF's photobleaching rates in the presence of the respective samples and standard, respectively, while I_{abs} and I_{abs}^{std} were the rates of light absorption by the samples and standard, respectively.

$$\Phi_\Delta = \Phi_\Delta^{Std}\frac{R\cdot I_{Abs}^{Std}}{R^{Std}\cdot I_{Abs}} \qquad (2)$$

Photo-irradiations were studied using a General Electric Quartz line lamp (300W). A 600 nm glass cut off filter (Schott) and a water filter were used to filter off ultraviolet and infrared radiations, respectively. An interference filter (Intor, 670 nm with a band width of 40 nm) was additionally placed in the light path before the sample. Light intensities were measured with a POWER MAX5100 (Molelectron detector incorporated) power meter.

For direct method, the calculation of the $^1O_2$ quantum yields was based on the detection of NIR $^1O_2$ luminescence by an optical method based on the comparison of single molecular oxygen phosphorescence produced by the Pc sample with that generated by the reference ZnPc in the near infrared region at 1276 nm. Φ_Δ values were calculated according to Equation 3.

$$\phi_{\Delta s} = \phi_{\Delta r}\frac{\eta_s^2 A_r I_s}{\eta_r^2 A_s I_r} \qquad (3)$$

In Eq. 3, $\Phi_{\Delta s}$ and $\Phi_{\Delta r}$ are the quantum yields of the sample and reference and η_s and η_r are refractive indexes of the solvents used for the measurements of the sample and reference. A_s and A_r are the absorbance of the sample and the reference, and I_s and I_r are the integrated areas under the emission spectra of the sample and the reference, respectively. The measurements were done by Horiba Jobin-Yvon Fluorometer with Hamamatsu NIR PMT 5509.

Electrochemical analyses: Electrochemical measurements were carried out on a CH Instruments 842B model work station. The setup was a conventional three-electrode cell equipped with a glassy carbon working electrode, platinum wire counter electrode, and $Ag/AgNO_3$ reference electrode. The glassy carbon electrode was polished routinely with 1 micron, 0,3 micron and 0.05 micron alumina powder/water slurry on pads before running experiments respectively. All measurements of samples were recorded as reported analyte concentration in 0.1 M $n\text{-}Bu_4NClO_4$ electrolyte solutions of dichloromethane. Solutions were deaerated by purging with argon for 5 min and kept under a blanket of argon during the experiments. All electrochemical measurements were performed at ambient temperature. Ferrocene was used as an internal reference, and all potentials were referenced to ferrocene/ ferrocenium (Fc/Fc^+) redox couple (E1/2: 0.480 V vs. SCE). All potentials as E1/2: (Epa + Epc)/2 were reported vs. saturated calomel electrode (SCE). Scan rate was 100 mV/s for all cyclic voltammetry (CV) experiments. The 3 mm-diameter glassy carbon working electrode (CHI104), non-aqueous Ag/Ag+ reference electrode with porous teflon tip (CHI112), platinum wire counter electrode (CHI115) and electrode polishing kit (CHI120) were purchased from CH Instruments. The supporting electrolyte, n-Bu4NClO4 was purchased from Acros Organics. Ferrocene was supplied by Fluka, $AgNO_3$ by Carlo Erba, and anhydrous Dichloromethane by Sigma Aldrich.

Electrochemical measurements were carried out using a glassy carbon working electrode in non-polar non-coordinating DCM medium, including TBAP as the electrolyte, to determine redox behavior of these Pc complexes. The half-wave potentials ($E_{1/2}$), anodic to cathodic peak potential separations (ΔEp), ratios of anodic to cathodic peak currents (Ipa/Ipc) and differences between the first oxidation and reduction potentials ($\Delta E_{1/2}$) for the redox processes of the complexes are listed in Table 3. The highest occupied molecular orbital (HOMO) and the lowest unoccupied molecular orbital (LUMO) energy gap levels of mono and double decker complexes were calculated using the characteristic oxidation and reduction values of ferrocene at -4.8 eV [5-7] in DCM (Table 3) with Equations **1** and **2**, respectively. Bu refler eklenmeli

$$E_{HOMO} = -\,[(E_{ox} - E_{1/2(ferrocene)}) + 4.8] \qquad \textbf{Eq. 1}$$

$$E_{LUMO} = -\,[(E_{red} - E_{1/2(ferrocene)}) + 4.8] \qquad \textbf{Eq. 2}$$

2. Synthetic Procedures

Phthalonitrile FN-Pox:To a solution of 0.9 g (0.004 mol) 4,5-dichlorophthalonitrile [8] in anhydrous Acetone (20 ml) l-mercapto-4,7,10-trioxaundecane [9] 2.8 g (0.015 mol) was added under argon. After stirring for 10 min, finely ground anhydrous K_2CO_3 (2.5 g, 0.018 mol) was added portion wise in 2h with efficient stirring. The reaction mixture was stirred under argon at room temperature for 24h. Then after filtration the solvent was evaporated then the combined extracts were purified by column chromatography on silica gel using dichloromethane as the eluent. The product is oily at room temperature. Yield: 1.03 g (%46.5), FT-IR (ATR): νmax (cm^{-1}), 3079, 2940-2840 (CH), 2229 (CN), 1566, 1459, 1350, 1272, 1228, 1101, 1027, 930, 849. ESI-MS: Calculated ($C_{22}H_{32}N_2O_6S_2$) $[M]^+$ 484.64 m/z, found $[M_+Na]^+$ 507.30 m/z. ^{1}H NMR (500 MHz, $CDCl_3$, δ ppm): 7.62 (s, 2H, Ar-H), 3.80 (t, 4H, OCH_2), 3.72-3.54 (m,16H, $S(OCH_2C)$), 3.38 (s, 6H, OCH_3), 3.22 (t, 4H, $S(CH_2)$. ^{13}C NMR (125 MHz, CDCl3, δ ppm): 143.95 (Ar-C), 129.27 (Ar-CH), 111.22 (Ar-CH), 115.50 (CN), 71.89, 70.75, 70.25, 69.34 (-CH2-), 59.04 (OCH3), 32.62 (SCH2).

Phthalonitrile FN-OH: 3 g (17.34 mmol) 4-nitrophthalonitrile was dissolved in 35 mL of dry DMF and was mixed for 5 min. under argon. After the temperature reached 40 °C 2.35 mL (17.34 mmol) 6-mercapto-1-hexanol was added to the mixture under argon atmosphere. After 1 h stirring, finely ground anhydrous K_2CO_3 (3.5 g (0.025 mol) was added portion wise in 1h with efficient stirring. The pink color reaction mixture was stirred for 3 days and finalized reaction by pouring mixture in an ice-bath. The aqueous phase was extracted with dichloromethane (3 x 50 rnl). The combined extracts were dried over sodium sulfate, the solvent was evaporated and the product was crystallized from EtOH and dried in vacuum. Yield: 0.9 g (% 20). FT-IR [(ATR) υmax/cm^{-1}]: 3332.9 (w) (CH2OH), 3139.4(w) (Ar C–H), 2930.7, 2890.3, 2860.6 (m) (Aliph-CH2), 2232.8 (m) (-CN), 1580.2 (s), 1473.3(s) , 1398.5(m), 1192.5(m), 1073.3 (s) , 831.6 (s) cm^{-1}. ^{1}H NMR (500 MHz, $CDCl_3$, ppm): δ 7.65 (d, 8.5 Hz, 1H), 7.56 (bs, 1H), 7.50 (8Hz, 1H), 3.67 (t, 7.25 Hz, 2H), 3.03 (t, 7.25 Hz, 2H), 1.76 (t, 7.25 Hz, 2H), 1.61 (t, 6.75 Hz, 3H), 1.53 (t, 7.25 Hz, 2H), 1.45 (m, 2H). ^{13}C NMR (125 MHz, $CDCl_3$, δ ppm): 147.3, 133.1, 129.9, 129.8, 116.2, 115.5, 115.1, 62.6, 32.4, 31.7, 28.5, 28.1, 25.2. ESI-MS m/z: 278.20 $[M+H_2O]^+$.

2,3,9,10,16,17,23,24-Octakis(4,7,10-trioxaundecane-1-sulfanyl) phthalocyanine (H_2PcPox)

Method A: This method consist of 2 steps; production of ZnPc first then removing of Zn metal to produce free Pc.

Method A-Step 1 (ZnPcPox): Phthalonitrile **FN-Pox** (1.3 g, 2.68 mol) and $Zn(OAc)_2$ (1.31 mol, 240 mg) are refluxed in dry DMAE (dimethylaminoethanol) (5 mL) overnight. The cooled reaction mixture was poured in boling n-hexane (50 mL), and the green oily product was purified on a silica gel column chromatography, eluted by dichloromethane/ethanol (20:1) mixtures of increasing polarity. Yield: 0.35 g (% 26). FT-IR (ATR): ν_{max} (cm^{-1}), 3055, 2918–2868(CH_2, CH_3), 1655 (C-N), 1592, 1370 (C-N), 1285, 1245, 1196, 1140–1067(C–O–C). MALDI-TOF (matrix: DHB): Calculated ($C_{88}H_{128}N_8O_{24}S_8Zn$) $[M]^+$ 2002 m/z, founded $[M]^+$ 2002.35 m/z. ^{1}H NMR (500 MHz, d_6-DMSO, δ ppm): 9.10 (s, 8H, ArH), 3.66 (t, 16H, SCH_2), 3.98 (t, 16H, OCH_2), 3.74 (t, 16H, OCH_2), 3.62 (t, 16H, OCH_2), 3.51(t, 16H, OCH_2), 3.35 (t, 16H, OCH_2), 3.12 (s, 24H, OCH_3). UV-Vis ($CHCl_3$), λ_{max}/nm: 633, 663, 691, 723

Method A-Step 2 (H_2PcPox): Demetallation of 300 mg ZnPc derivate (**ZnPcPox**) was occurred in 5 mL pyridine and pyridium chloride (1.5 g) by stirring 24 hr at 90 °C. Pyridine was evaporated under vacuum at low pressure. Metal free phthalocyanine was purified on a silica gel column chromatography, eluted by dichloromethane/ethanol (20:1) mixture. Yield: 0.21 g (% 72). FT-IR (ATR): νmax (cm^{-1}), 3291(NH), 2980-2864 (CH), 1591 (C=N) 1455, 1416,1399, 1352, 1287, 1196, 1095-1022 (C-O-C). MALDI-TOF (matrix:

DHB): Calculated ($C_{88}H_{130}N_8O_{24}S_8$) $[M]^+$ 1937 m/z, founded $[M]^+$ 1937.99 m/z. ^1H NMR (500 MHz, d_6-DMSO, δ ppm): 7.95 (s, 8H, ArH), 4.05 (t, 16H, SCH_2), 3.78 (t, 16H, OCH_2), 3.56-3.41 (t, 48H, OCH_2), 3.17 (s, 24H, OCH_3). UV-Vis ($CHCl_3$), ^{13}C-NMR: (125 MHz, d_6-DMSO, δ ppm): 139.47(ArC), 132.08(ArC), 119.70(ArC), 109.99(ArC), 71.75(OCH2), 70.45(OCH_2), 70.39(OCH_2) , 70.22(OCH_2) , 69.42(OCH_2), 58.48(OCH_2), 33.55(OCH_3). UV-Vis ($CHCl_3$) λ_{max}/nm: 636, 666, 698, 728

Method B (H_2PcPox): This method based on insitu two reactions; Li-template assisted tetramerisation, and insitu removal of the lithium ions by acidic treatments. The compound (**H_2PcPox**) was obtained as byproduct during synthesis of asymmetric phthalocyanine (**H_2PcAB_3OH**). In 10 mL reaction flask 0.03 g (0.113 mmol) **FN-OH** and 0.85 g (1.7 mmol, 15 eqv.) **FN-Pox** were dissolved in 3 mL dry DMAE under argon atmosphere. Some small peaces of Li granules were added for tetramerisation of phthalonitrile moieties with high ratio. Also some drops of DBU was added. The reaction mixture was stirred at 140 °C for 5 hr. After cooling the mixure was poured in 5 mL boiling hexane. By silica gel column chromatography, eluted by dichloromethane/ethanol (15:1) mixture **H_2PcAB_3OH** was eluted as target product (70 mg, yield 35%), **H_2PcPox** 140 mg, (yield 63%) as main product were eluted from reaction. **H_2PcAB_3OH** FT-IR (ATR): ν_{max} (cm^{-1}), 3475 (OH), 2914–2864(CH_2, CH_3), 1596 (C-N), 1285, 1197, 1101–1017(C–O–C). MALDI-TOF (matrix: DHB): Calculated ($C_{80}H_{114}N_8O_{19}S_7$) $[M]^+$ 1716.011 m/z, founded $[M]^+$ 1716.228 m/z. UV-Vis ($CHCl_3$), UV-Vis (EtOH) λ_{max}/nm: 633, 665, 701, 730

Symmetric mono- lanthanide phthalocyanines (LnPcPox(OAc); Ln:Lu(III) or Eu(III))

(LnPcPox(OAc)): For insertion of lutetium complex, lutetium acetate $Lu(AcO)_3$ (0.042 g, 0.12 mmol) was added to a stirred mixture of metal-free phthlocyanine (0.200 g, 0.103 mmol) (**H_2PcPox)**or for Europium complex; europium acetate $Eu(AcO)_3$ (0.084 g, 0.25 mmol), metal-free phthlocyanine **(H_2PcPox)** (0.38 g, 0.196 mmol) and 2-3 drops of organic base DBU (1,8-diazabicyclo[5,4,0] undec-7-ene) in freshly distilled dry *o*-DCB (o-dichlorobenzene) (3 mL) at 180 °C under argon. The reaction mixture was left for 3-4 h at this temperature and controlled by TLC. After it cooled, the solution was poured in 50 ml n-hexane. Purification of oily green product was done by silica gel column, elution with dichloromethane/ethanol (20:1) mixture. Yield: 0.200 g (% 89) for Lu-complexand Yield: 0.320 g (% 75.9) for Eu-complex.

(LuPcPox(OAc)): FT-IR (ATR): νmax (cm^{-1}), 3055, 2918–2868(CH_2, CH_3), 1655 (C-N), 1592, 1370 (C-N), 1285, 1245, 1196, 1140–1067(C–O–C). MALDI-TOF (matrix: DIT): Calculated ($C_{90}H_{130}LuN_8O_{26}S_8$) $[M]^+$ 2172.51 m/z, founded $[M\text{-}AcO) + DIT]^+$ 2338.91 m/z.UV-Vis ($CHCl_3$), λmax/nm: 373, 633, 706.

(EuPcPox(OAc)): FT-IR (ATR): νmax (cm^{-1}), 2918–2868(CH_2, CH_3), 1591, 1365 (C-N), 1281, 1246, 1198, 1100–1064(C–O–C). MALDI-TOF (matrix: DIT): Calculated ($C_{90}H_{130}EuN_8O_{26}S_8$) $[M]^+$ 2149.5 m/z, founded $[M\text{-}AcO) + DIT]^+$ 2315.54 m/z. UV-Vis ($CHCl_3$), λ_{max}/nm: 545, 635, 705.

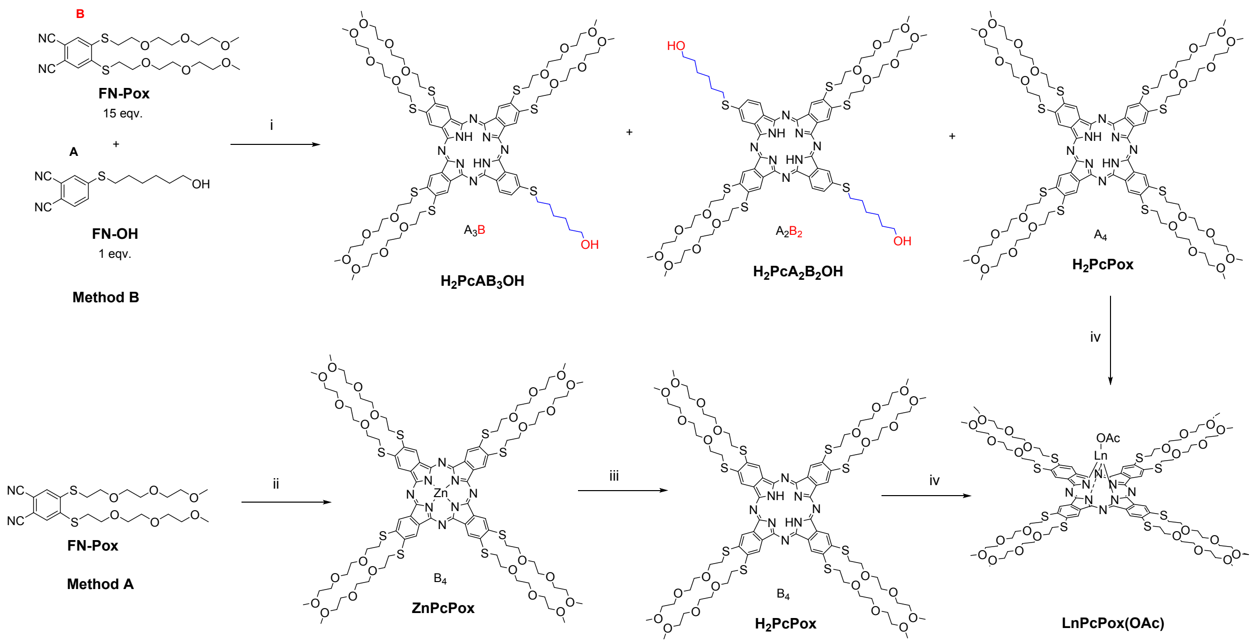

Scheme S1. Synthetic route for mono Lu(III) and Eu(III) phthalocyanine complexes (Ln(III)A_4Pc, Ln=Lu or Eu). i) Li, DMAE, DBU, reflux, under argon, ii) $Zn(OAc)_2$, DMAE, DBU, reflux (iii) pyridinium hydrochloride, pyridine, 90°C, 24h (iv) $Ln(AcO)_3$, *o*-DCB, reflux.

3. FT-IR, NMR and Mass Spectra of Compounds

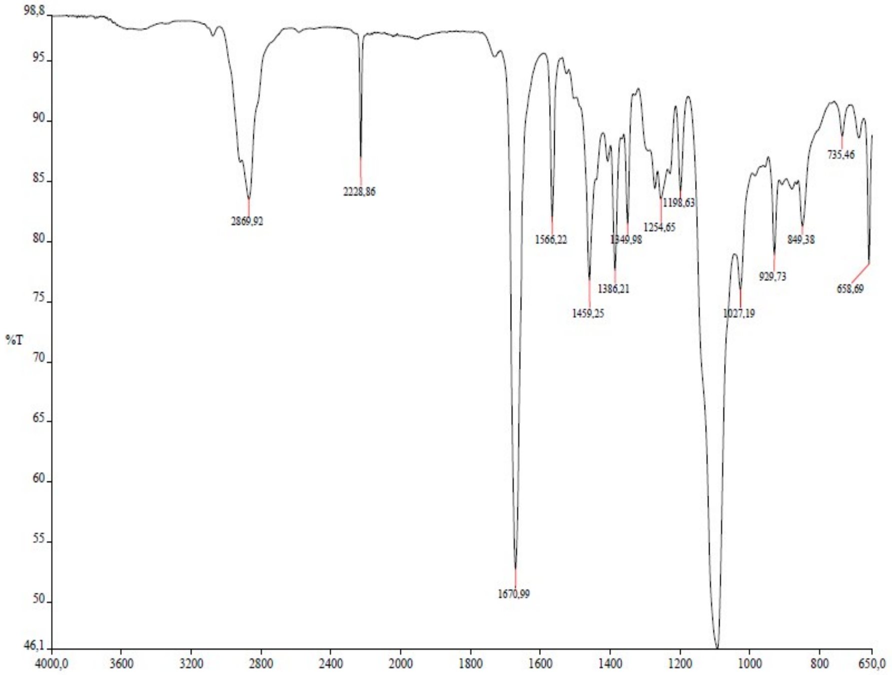

Figure S1 FT-IR spectrum of phthalonitrile **FN-Pox**

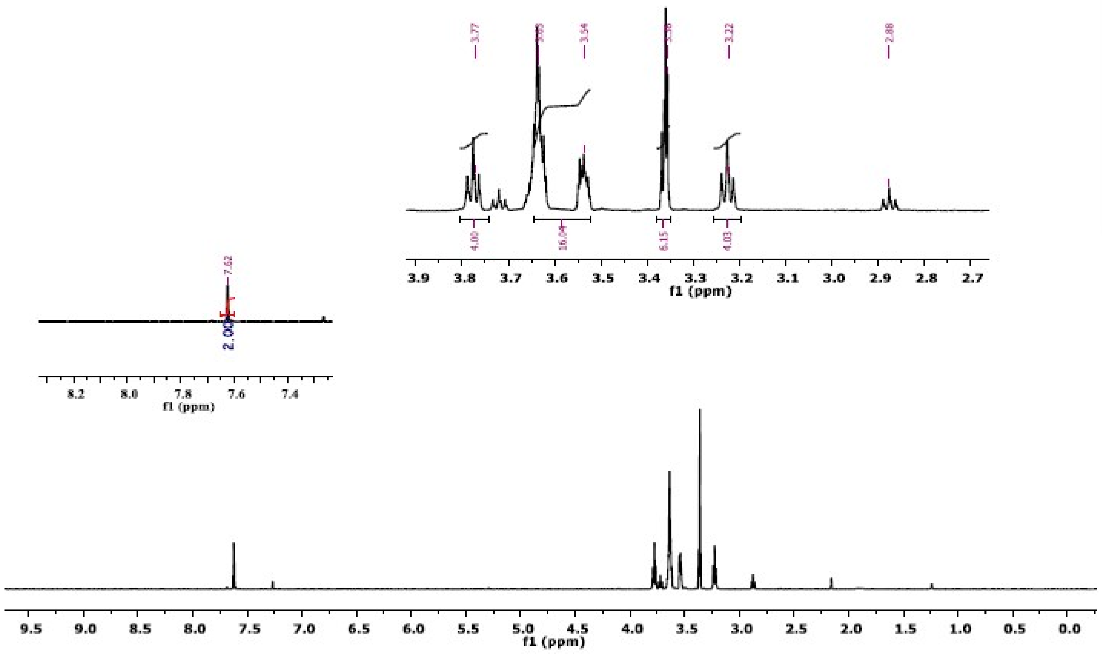

Figure S2 ^{1}H-NMR spectrum of phthalonitrile **FN-Pox** in CDCl3

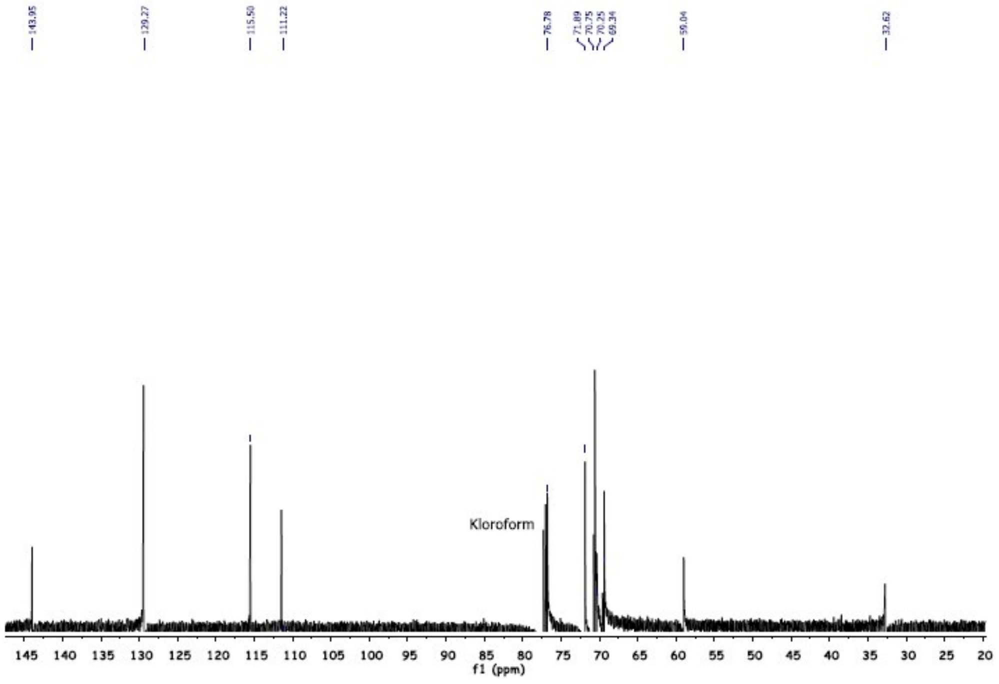

Figure S3 ^{13}C-NMR spectrum of phthalonitrile **FN-Pox** in $CDCl_3$

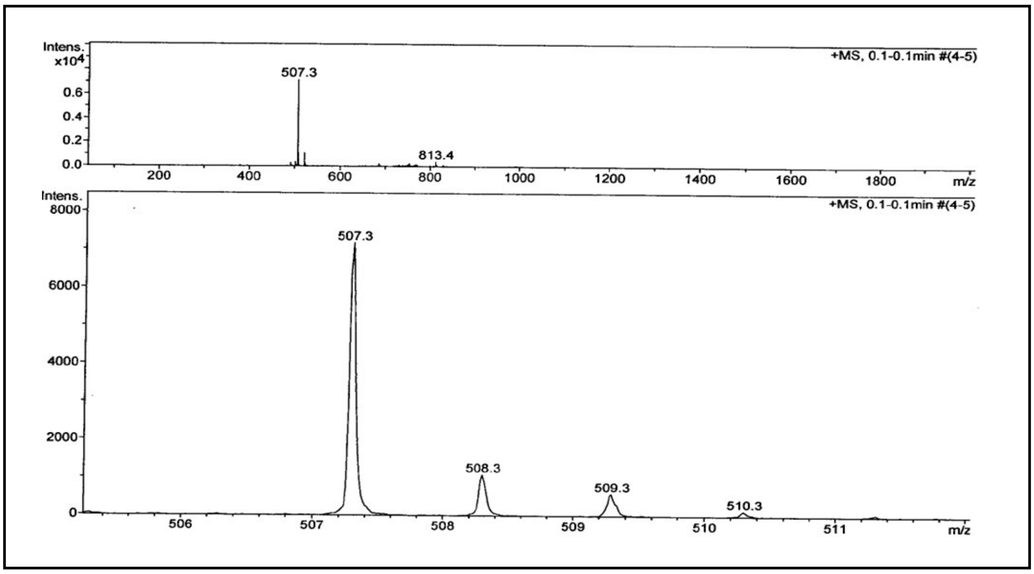

Figure S4 Mass spectrum (ESI) of phthalonitrile **FN-Pox**

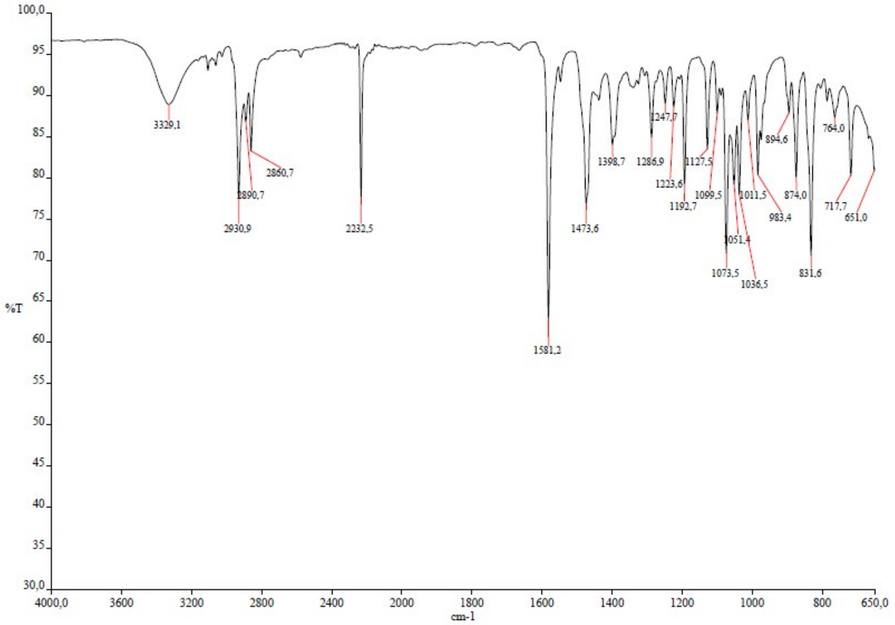

Figure S5 FT-IR spectrum of **FN-OH**

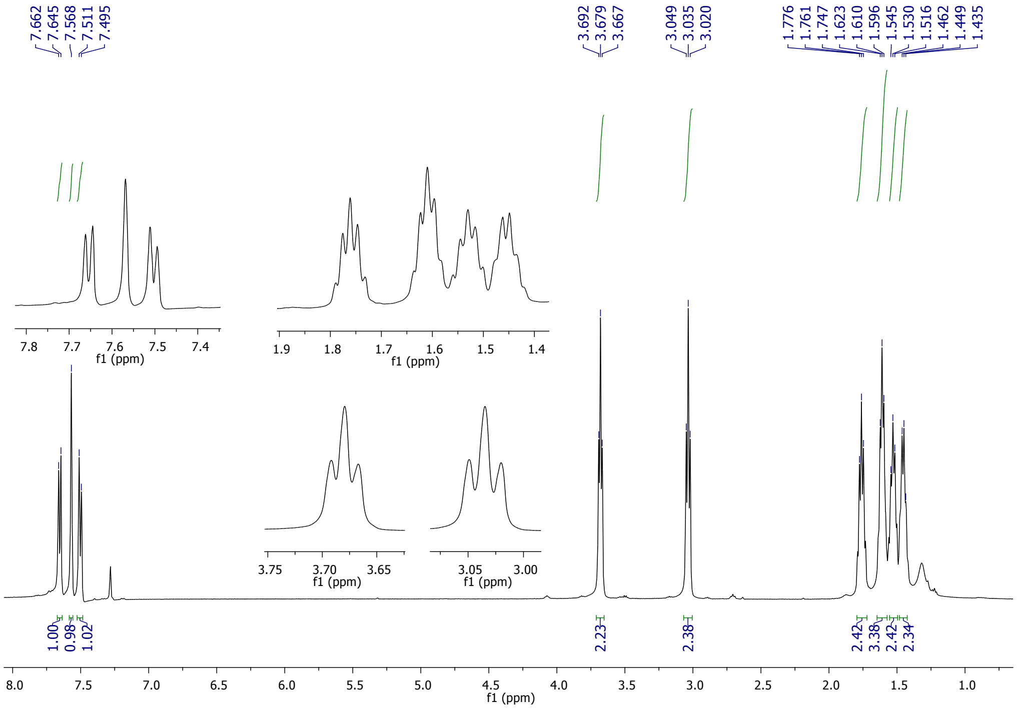

Figure S6 ^{1}H- NMR spectrum of **FN-OH** in $CDCl_3$

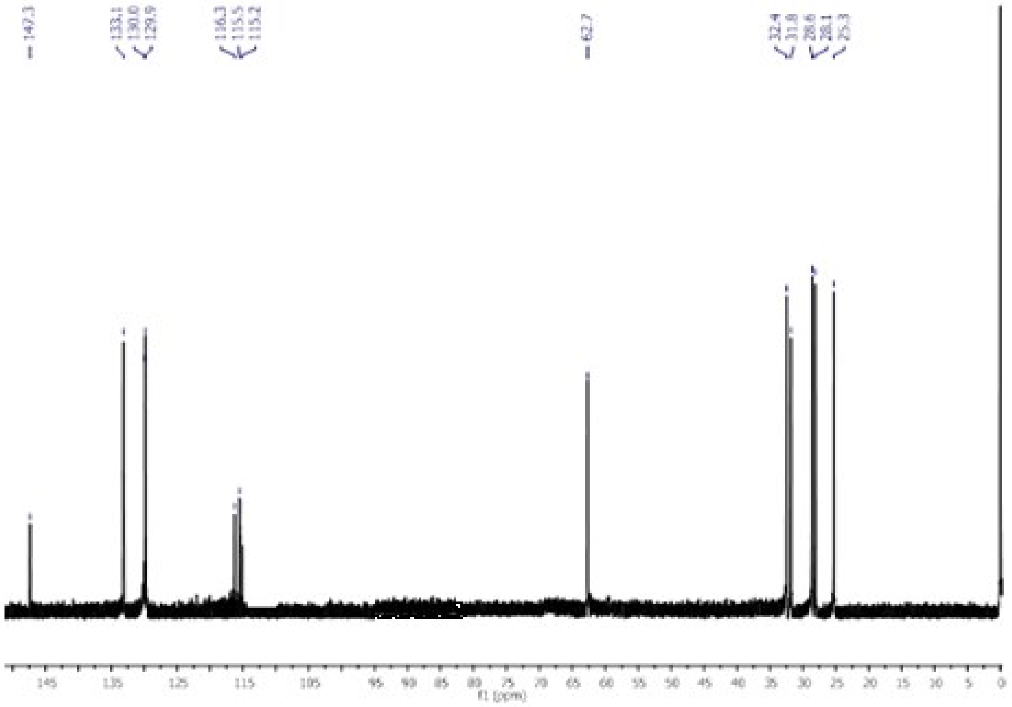

Figure S7 ^{13}C- NMR spectrum of **FN-OH** in $CDCl_3$

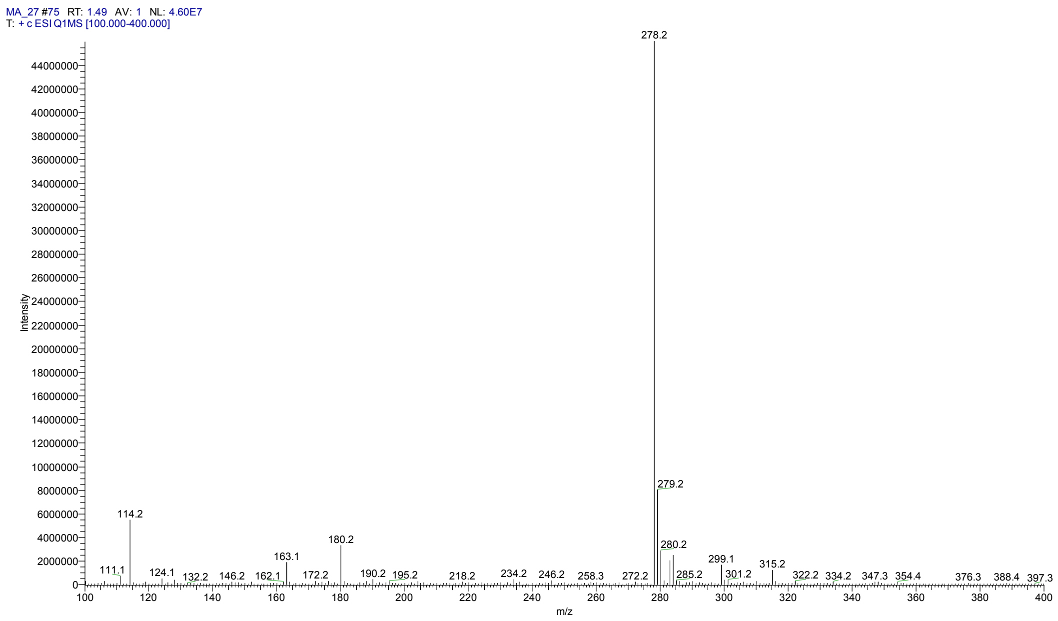

Figure S8 mass spectrum of **FN-OH**

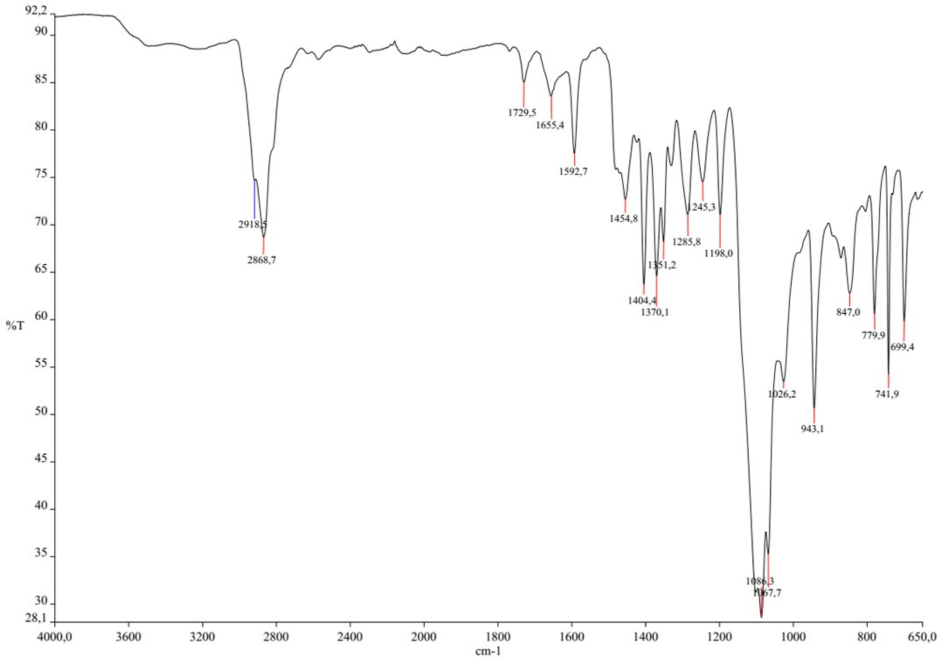

Figure S9 FT-IR spectrum of **ZnPcPox**

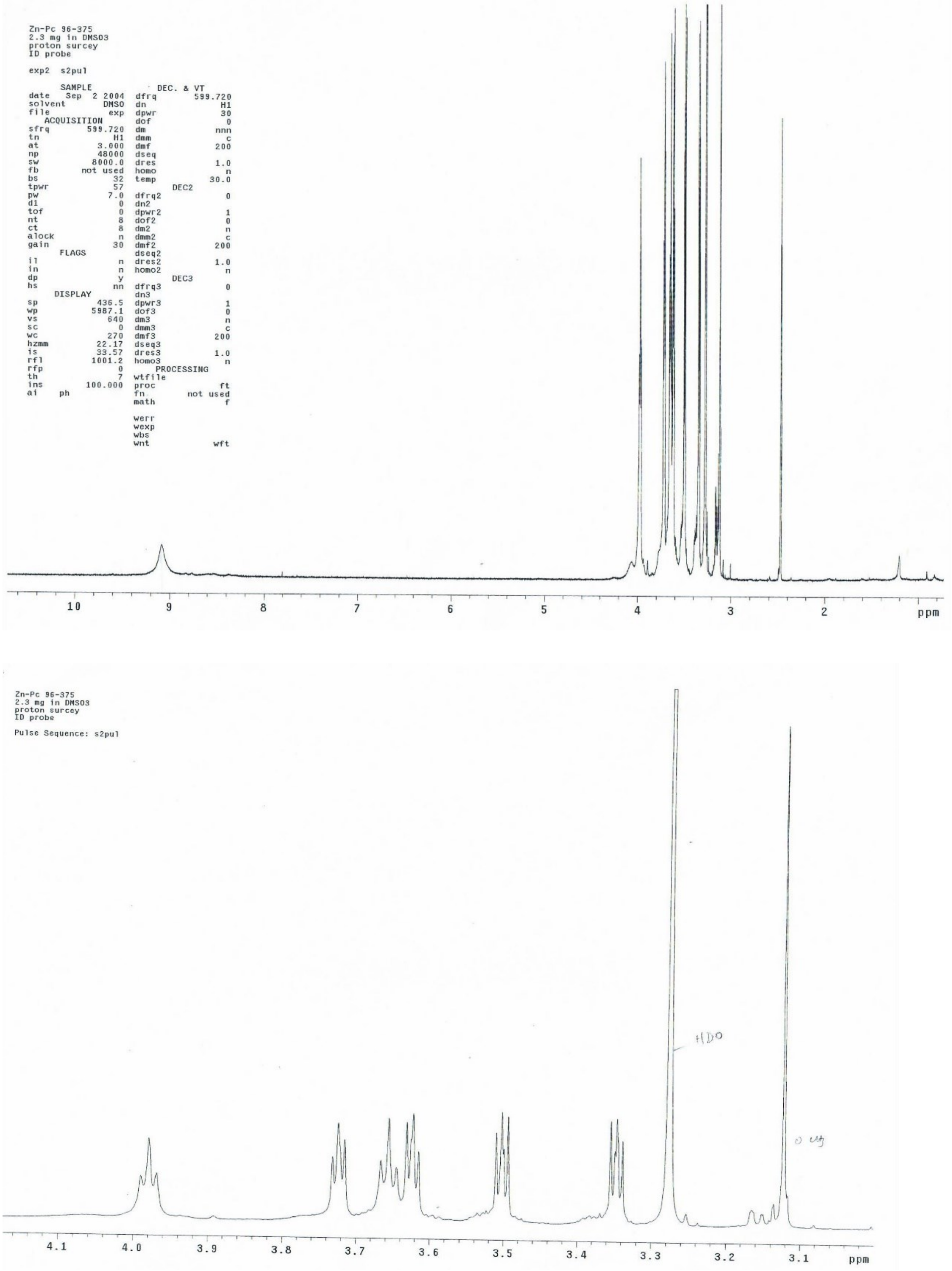

```
Zn-Pc 96-375
2.3 mg in DMSO3
proton surcey
ID probe

exp2  s2pul

      SAMPLE              DEC. & VT
date   Sep  2 2004  dfrq        599.720
solvent        DMSO dn               H1
file            exp dpwr             30
   ACQUISITION      dof               0
sfrq        599.720 dm              nnn
tn               H1 dmm               c
at            3.000 dmf             200
np            48000 dseq
sw           8000.0 dres            1.0
fb         not used homo              n
bs               32 temp           30.0
tpwr             57           DEC2
pw              7.0 dfrq2             0
d1                0 dn2
tof               0 dpwr2             1
nt                8 dof2              0
ct                8 dm2               n
alock             n dmm2              c
gain             30 dmf2            200
      FLAGS         dseq2
il                n dres2           1.0
in                n homo2             n
dp                y           DEC3
hs               nn dfrq3             0
     DISPLAY        dn3
sp            436.5 dpwr3             1
wp           5987.1 dof3              0
vs              640 dm3               n
sc                0 dmm3              c
wc              270 dmf3            200
hzmm          22.17 dseq3
is            33.57 dres3           1.0
rfl          1001.2 homo3             n
rfp               0       PROCESSING
th                7 wtfile
ins         100.000 proc             ft
ai     ph           fn         not used
                    math              f

                    werr
                    wexp
                    wbs
                    wnt             wft
```

```
Zn-Pc 96-375
2.3 mg in DMSO3
proton surcey
ID probe

Pulse Sequence: s2pul
```

Figure S10 ^{1}H -NMR spectrum of **ZnPcPox**

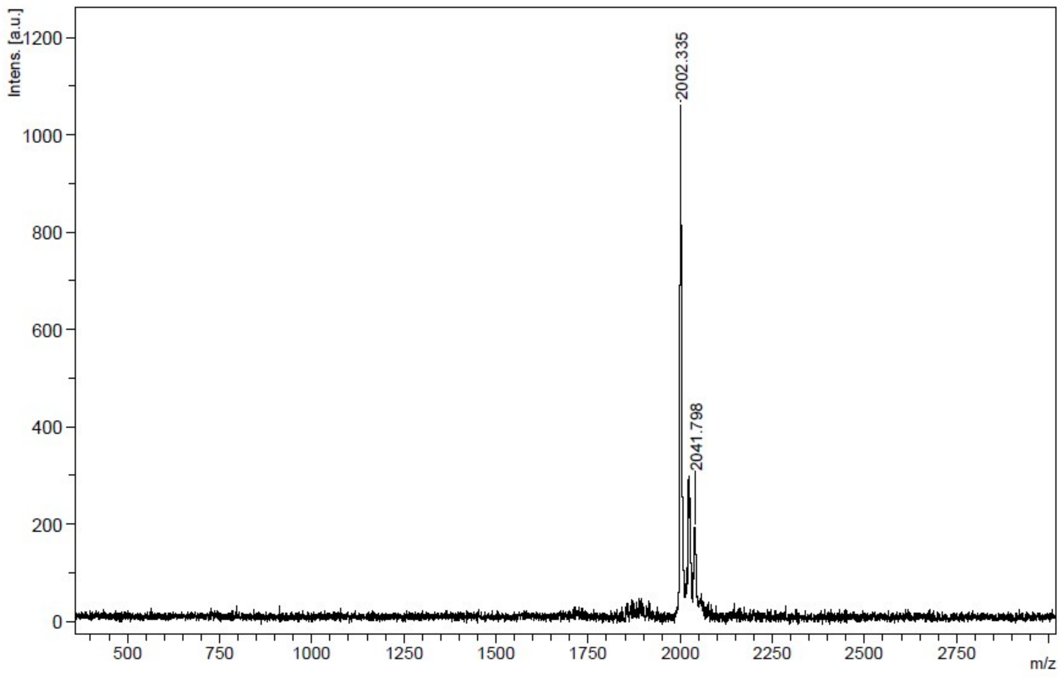

Figure S11 Mass spectrum of **ZnPcPox**

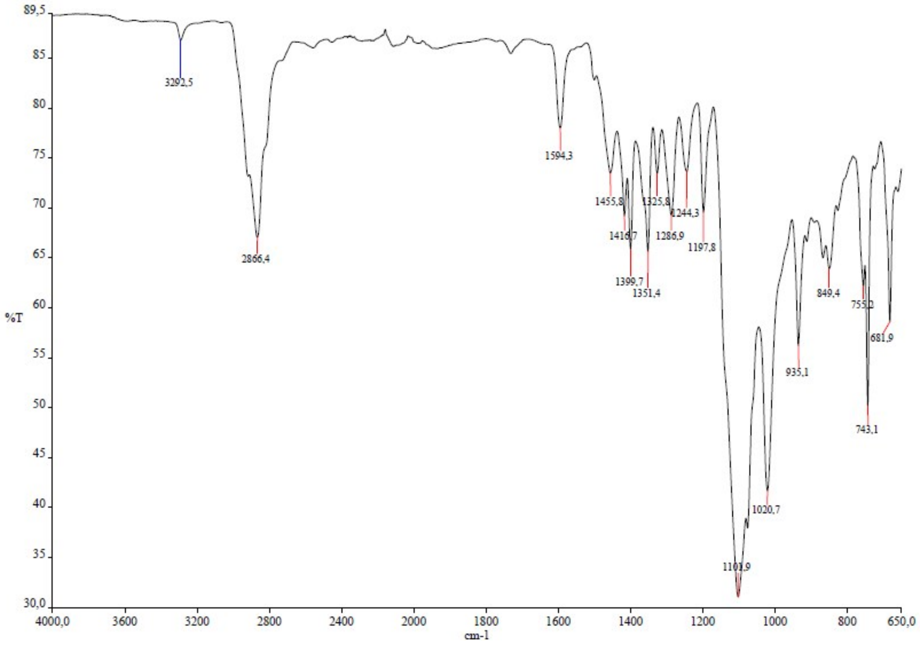

Figure S12 FT-IR spectrum of **H_2PoxPc**

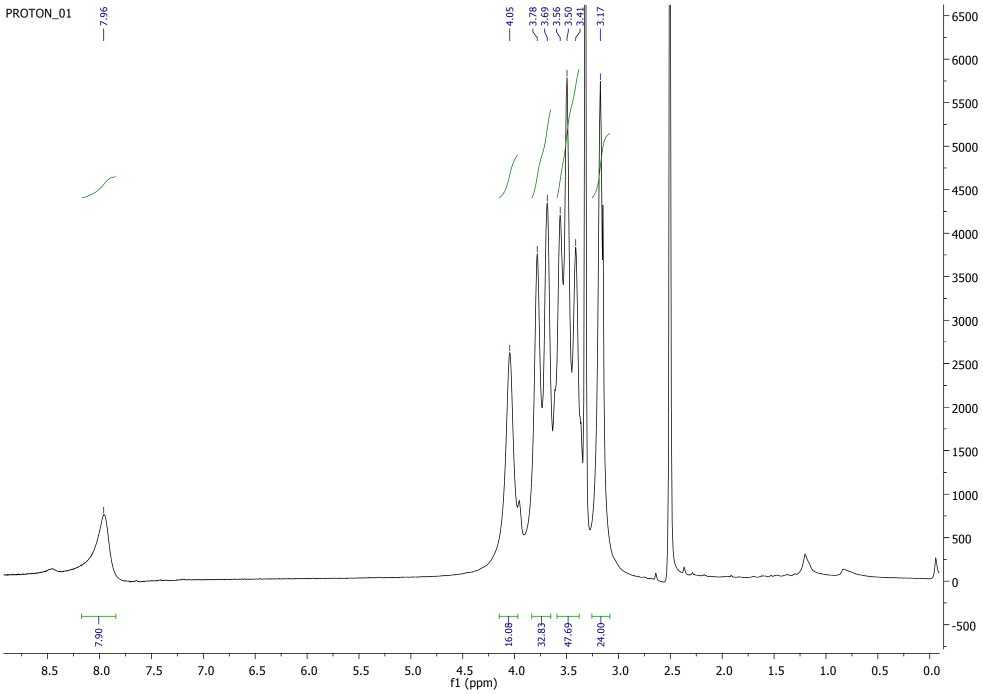

Figure S13 ^{1}H-NMR spectrum of **H_2PoxPc**

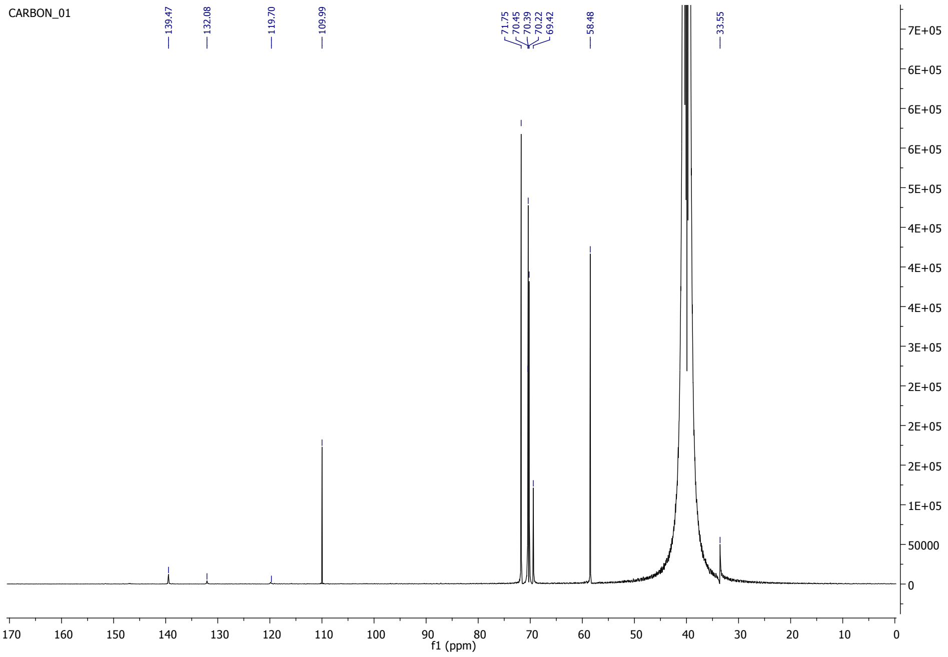

Figure S14 ^{13}C-NMR spectrum of **H_2PoxPc**

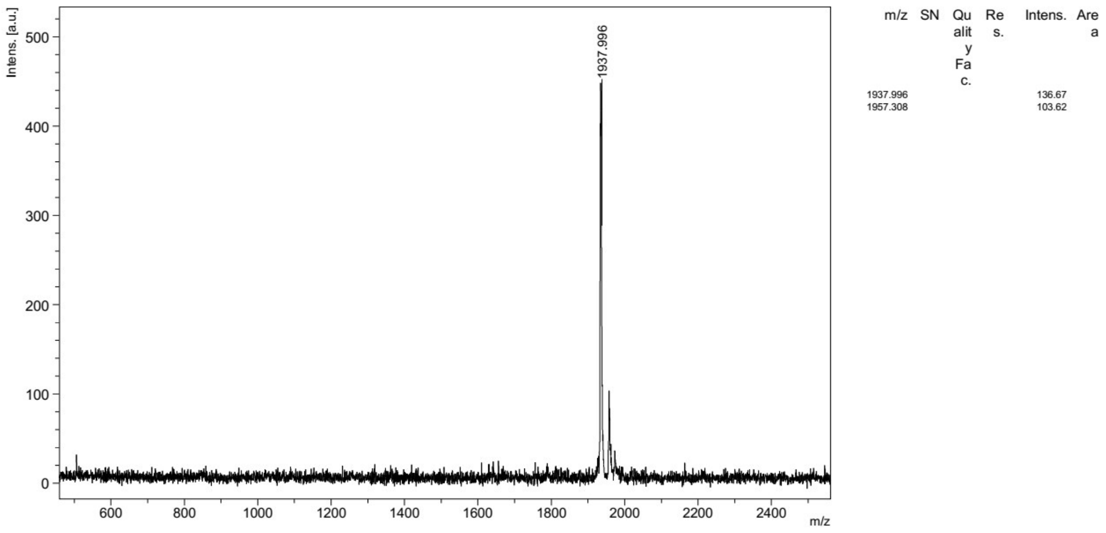

m/z	SN	Quality Fac.	Res.	Intens.	Area
1937.996				136.67	
1957.308				103.62	

Figure S15 Mass spectrum of $\mathbf{H_2PoxPc}$

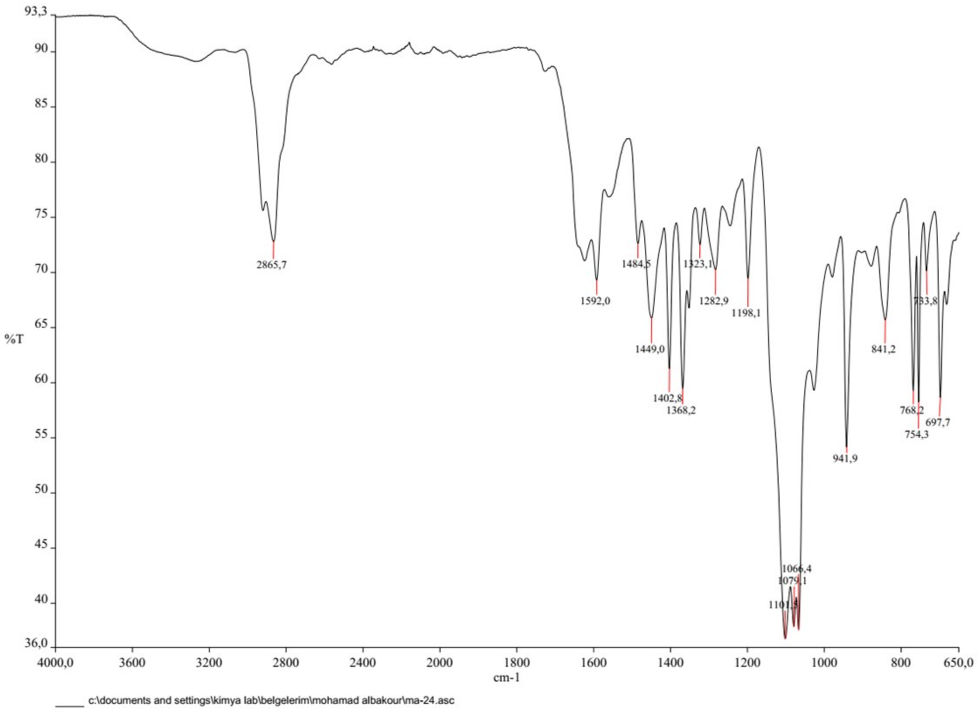

Figure S16 FT-IR spectrum of **LuPcPox(OAc)**

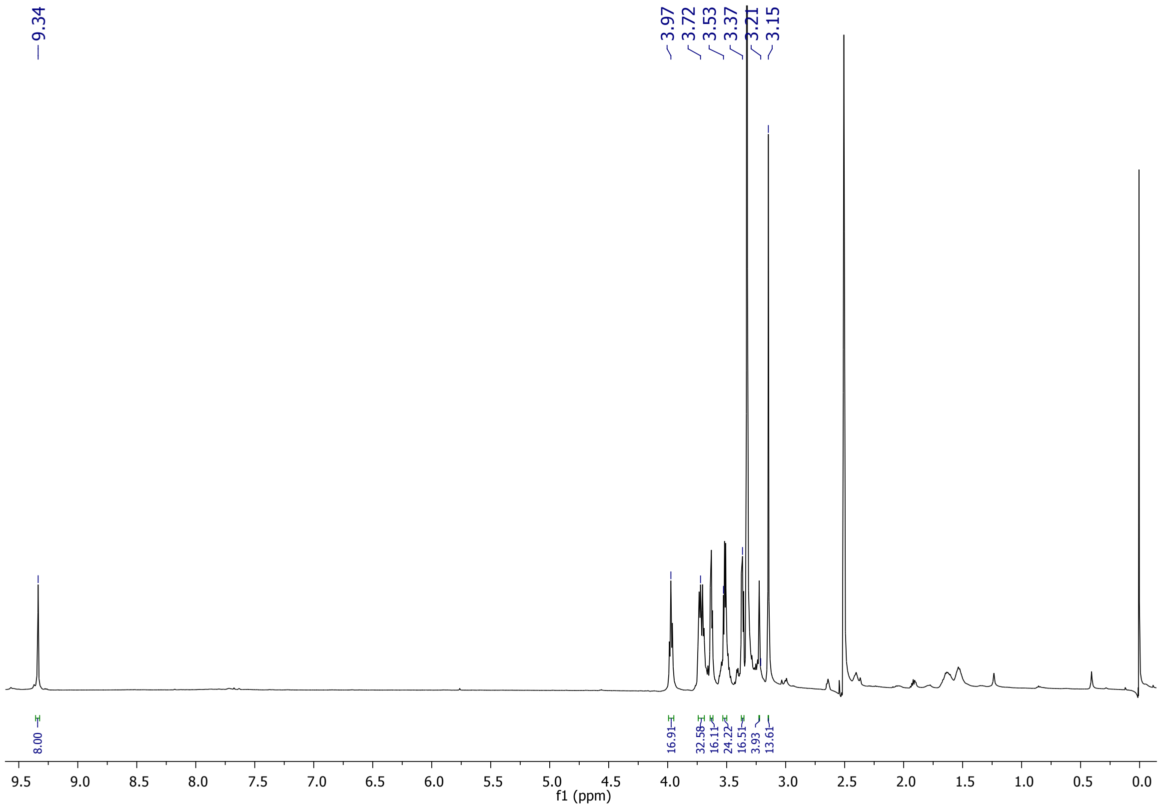

Figure S17 ^{1}H-NMR spectrum of **LuPcPox(OAc)**

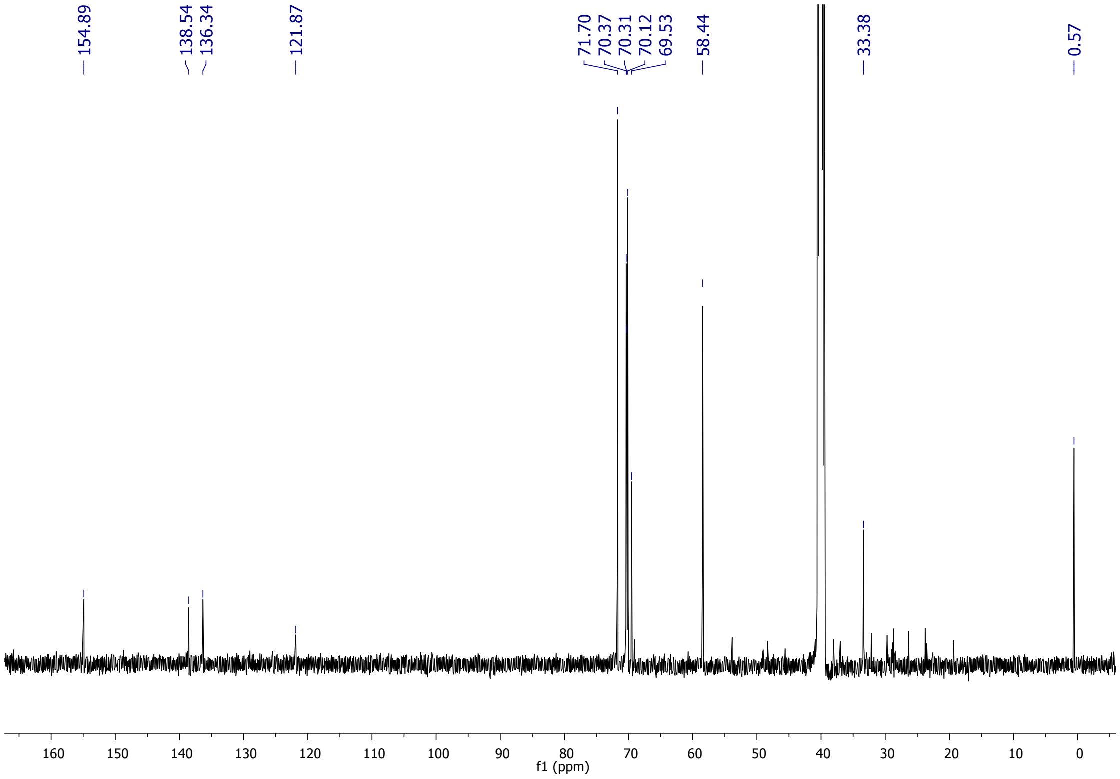

Figure S18 ^{13}C-NMR spectrum of **LuPcPox(OAc)**

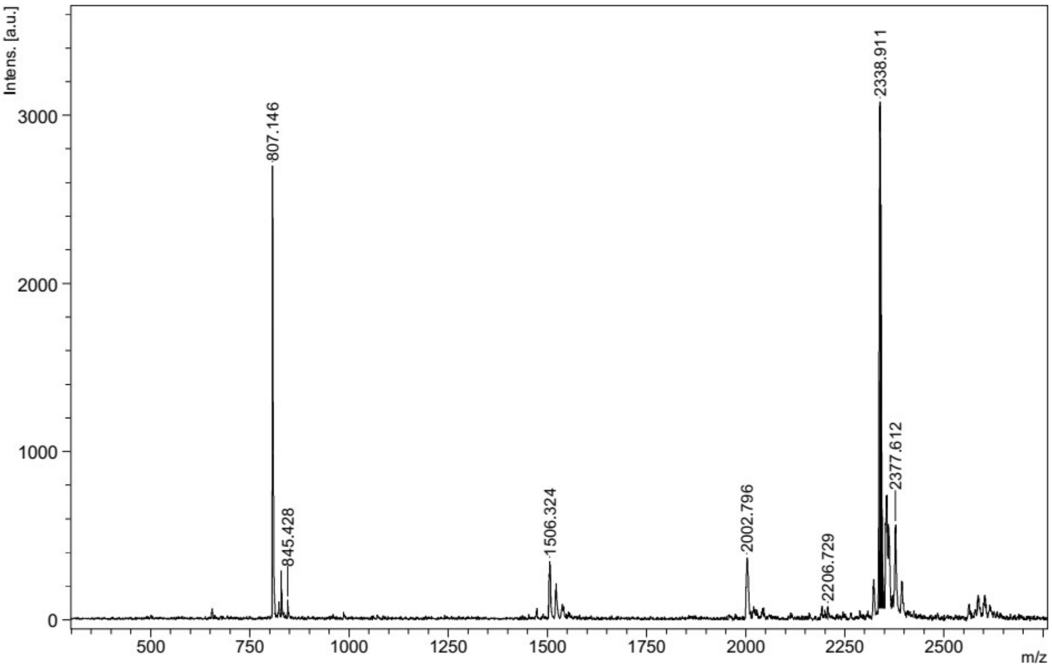

Figure S19 Mass spectrum of **LuPcPox(OAc)**

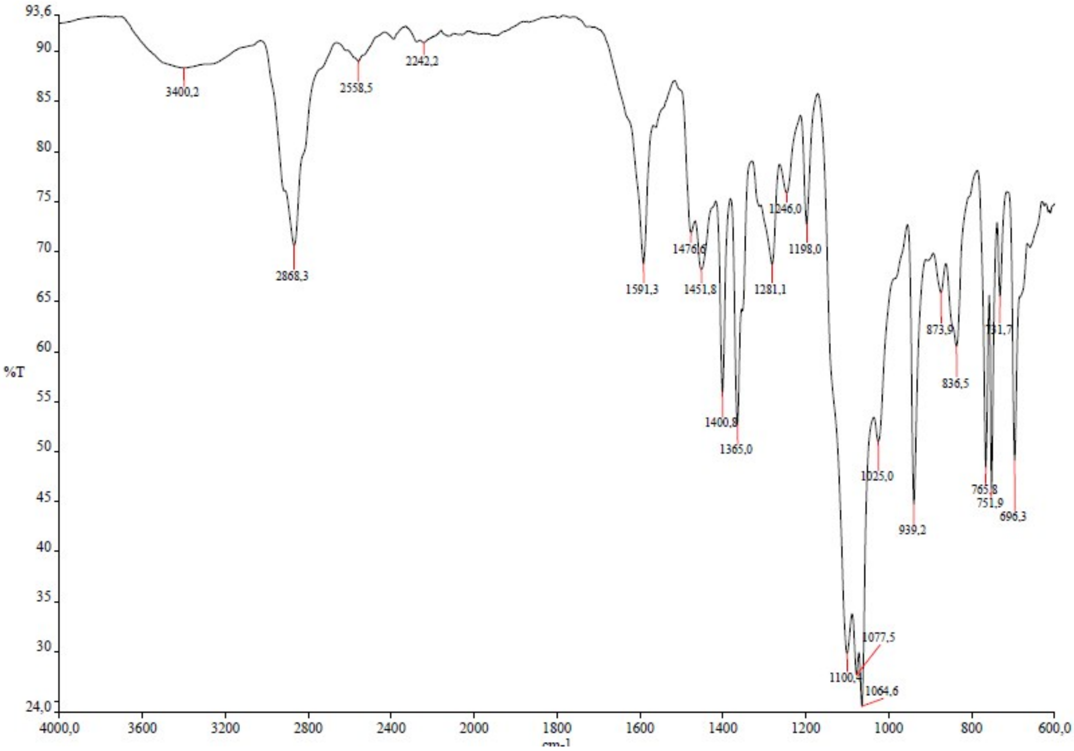

Figure S20 FT-IR spectrum of **EuPcPox(OAc)**

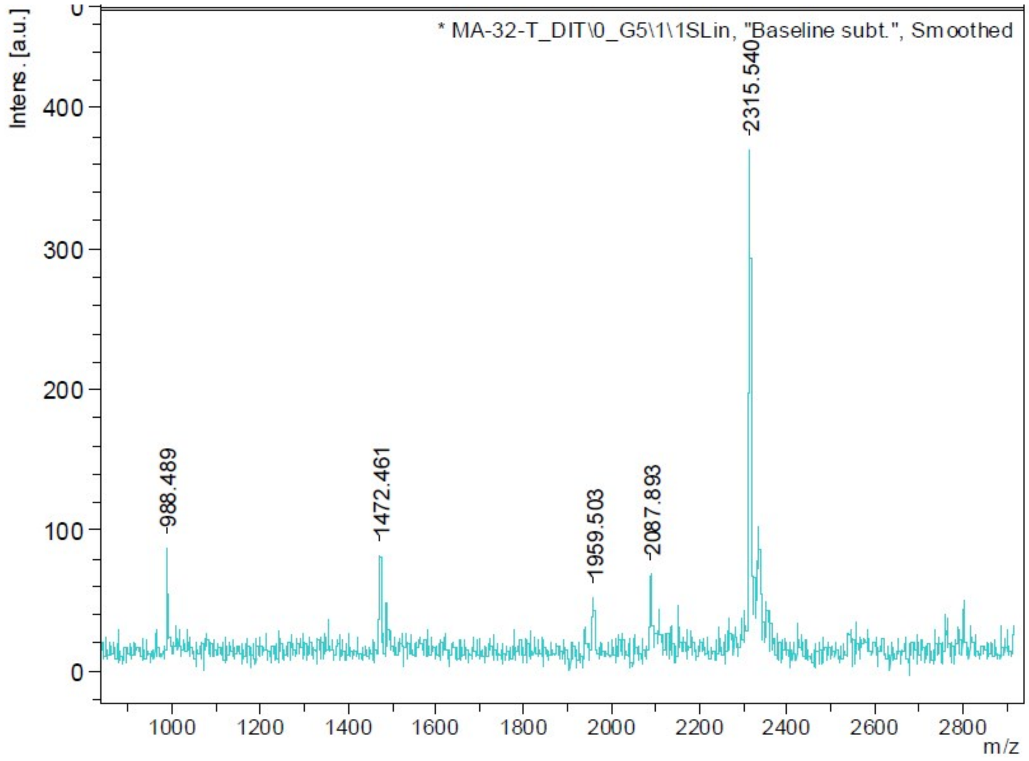

Figure S21 Mass spectrum of **EuPcPox(OAc)**

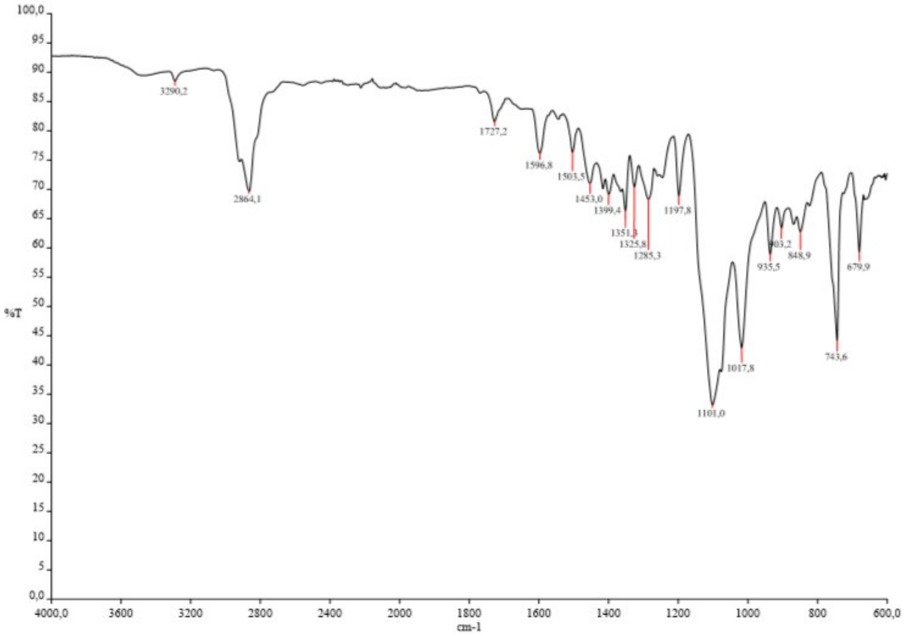

Figure S22 FT-IR spectrum of **H_2PcAB_3OH**

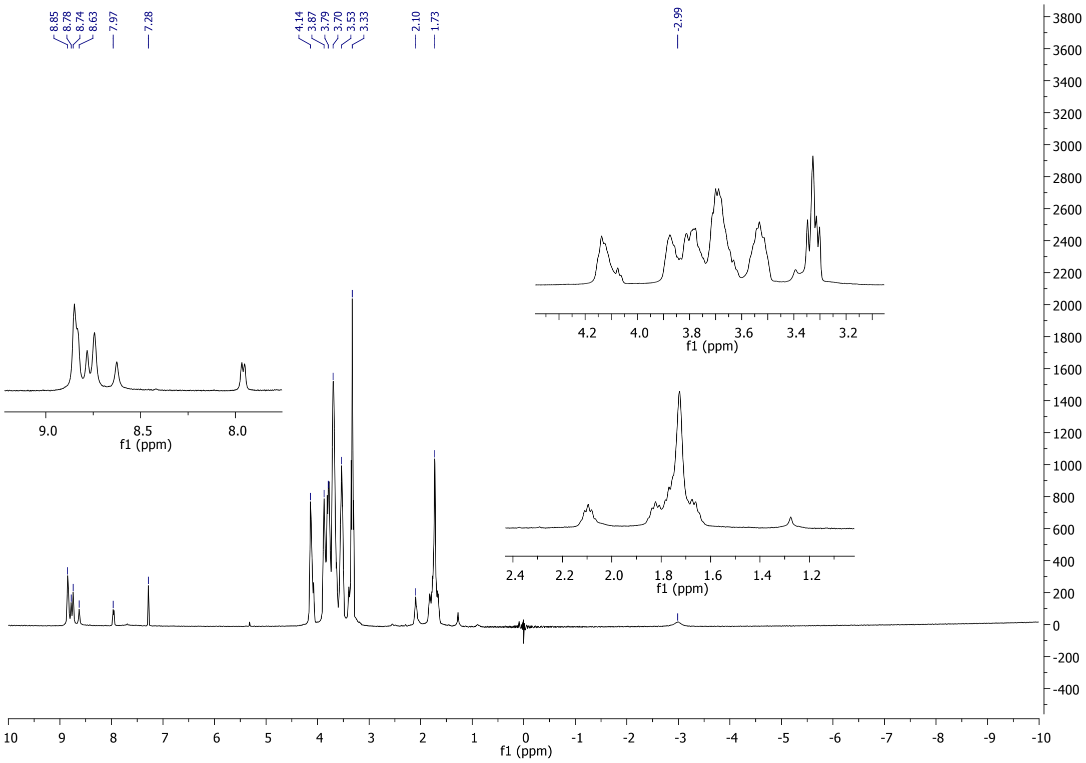

Figure S23 ^{1}H-NMR spectrum of **H_2PcAB_3OH**

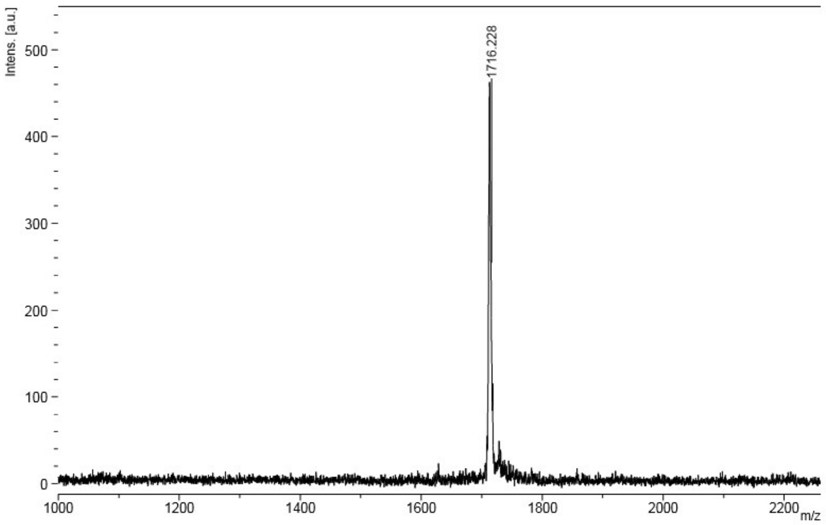

Figure S24 Mass spectrum of **H_2PcAB_3OH**

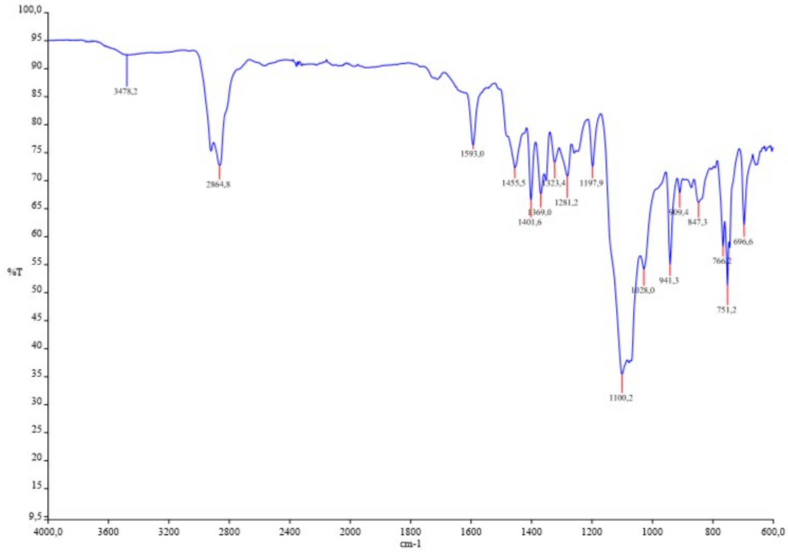

Figure S25 FT-IR spectrum of **LuPc(Pox)[Pc’(AB$_3$OH)]**

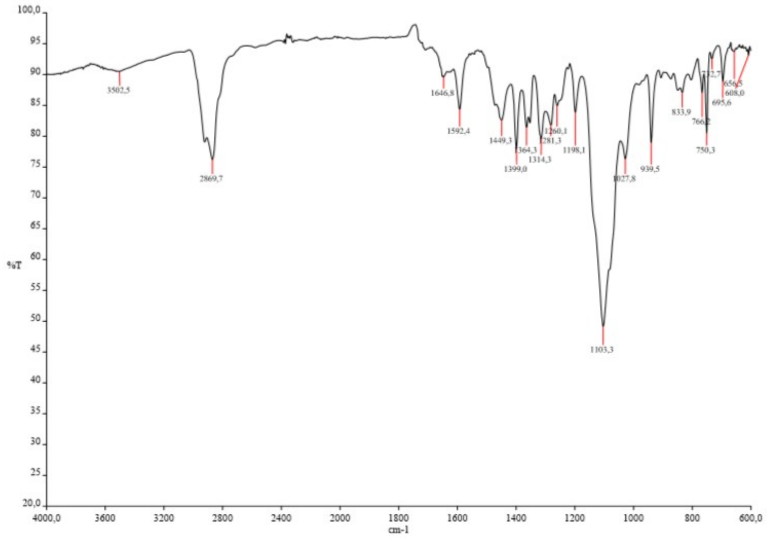

Figure S26 FT-IR spectrum of **EuPc(Pox)[Pc’(AB$_3$OH)]**

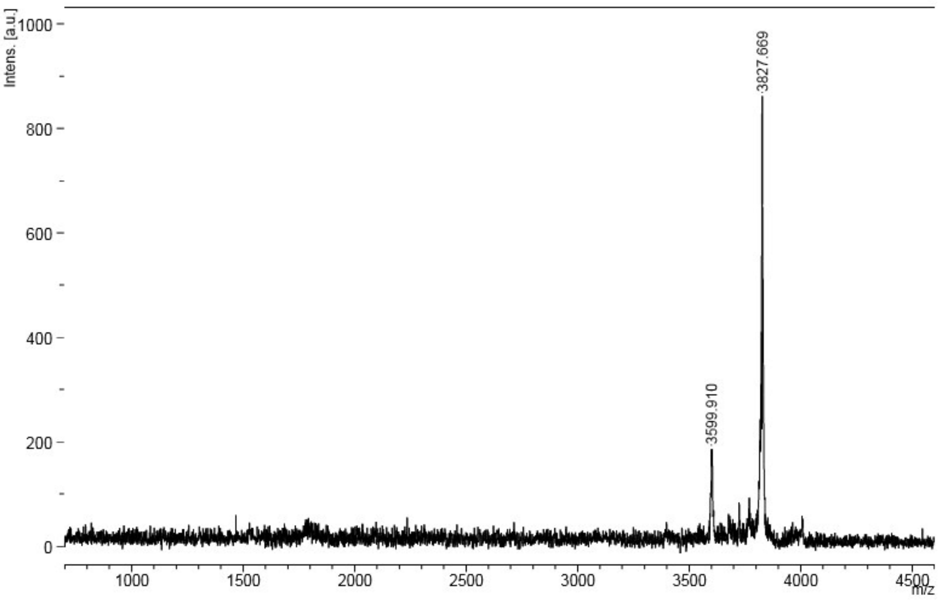

Figure S27 Mass spectrum of **LuPc(Pox)[Pc'(AB$_3$OH)]**

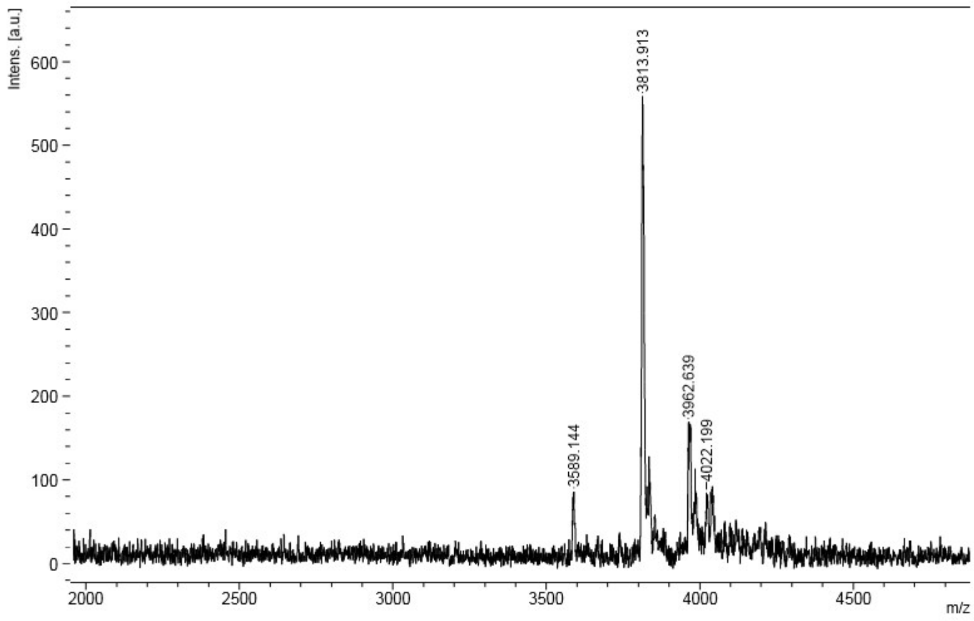

Figure S28 Mass spectrum of **EuPc(Pox)[Pc'(AB$_3$OH)]**

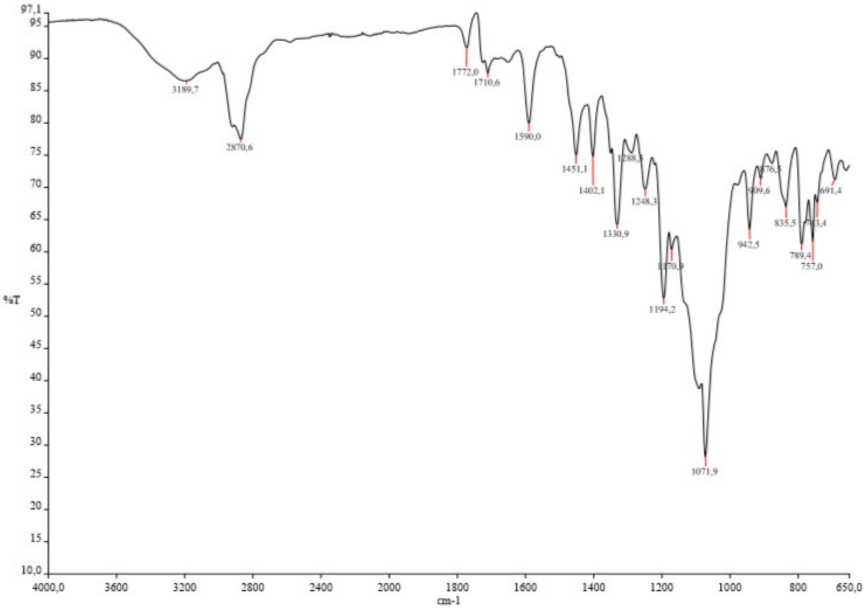

Figure S29 FT-IR spectrum of **LuPc(Pox)[Pc'(AB$_3$Mes)]**

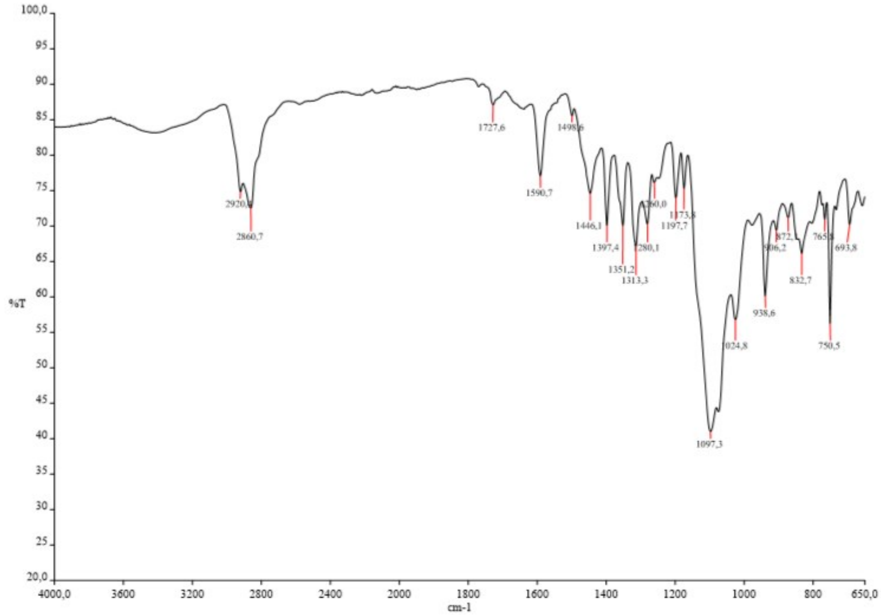

Figure S30 FT-IR spectrum of **EuPc(Pox)[Pc'(AB$_3$Mes)]**

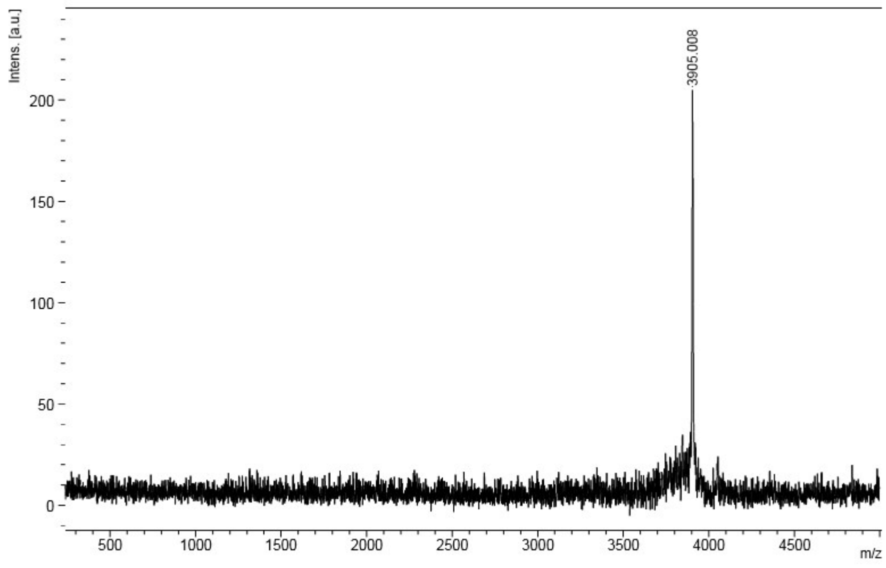

Figure S31 Mass spectrum of **LuPc(Pox)[Pc’(AB$_3$Mes)]**

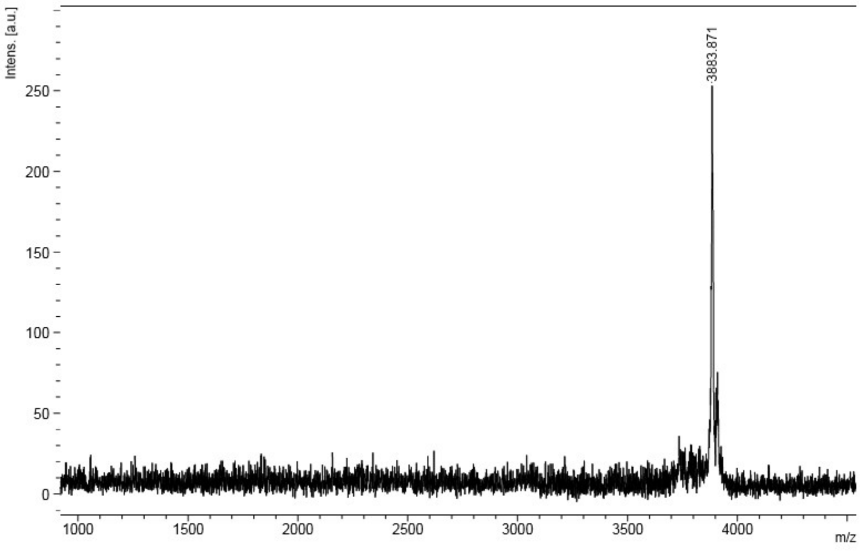

Figure S32 Mass spectrum of **EuPc(Pox)[Pc’(AB$_3$Mes)]**

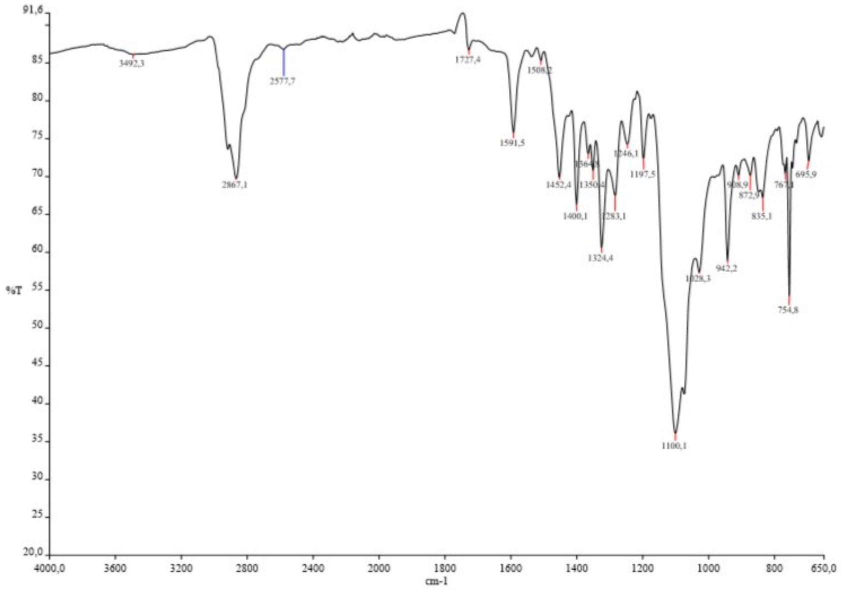

Figure S33 FT-IR spectrum of **LuPc(Pox)[Pc’(AB$_3$SH)]**

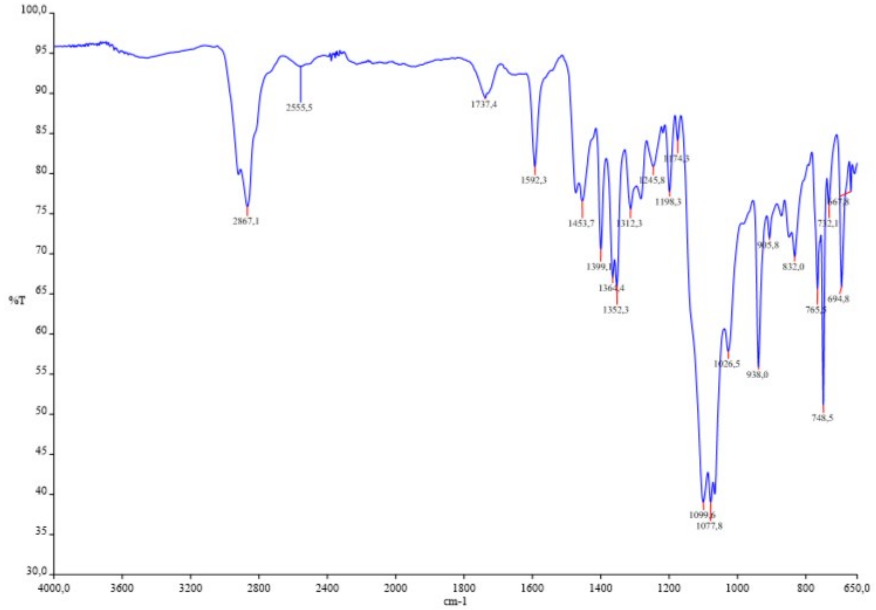

Figure S34 FT-IR spectrum of **EuPc(Pox)[Pc’(AB$_3$SH)]**

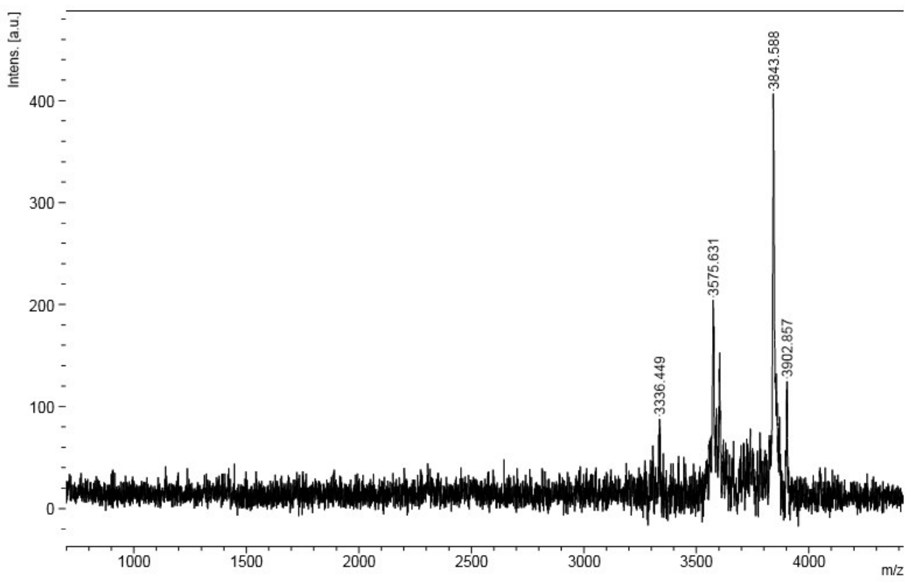

Figure S35 Mass spectrum of **LuPc(Pox)[Pc'(AB$_3$SH)]**

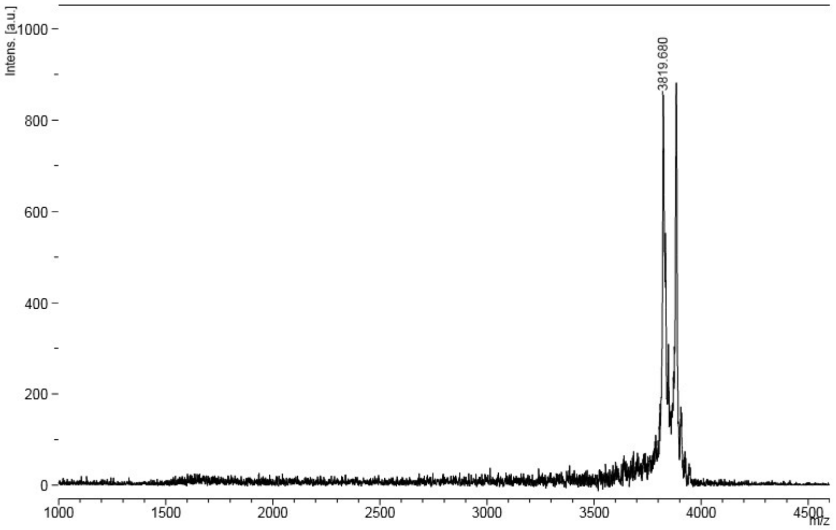

Figure S36 Mass spectrum of **LuPc(Pox)[Pc'(AB$_3$SH)]**

4. Absorption Spectroscopy

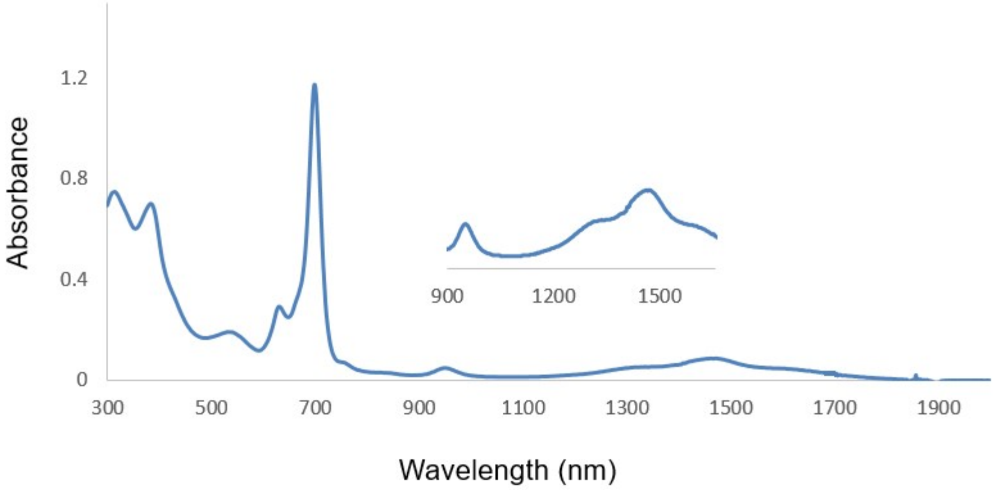

Figure S37 UV–vis and NIR spectra of **LuPc(Pox)[Pc’(AB_3OH)]** in neutral state in $CHCl_3$.

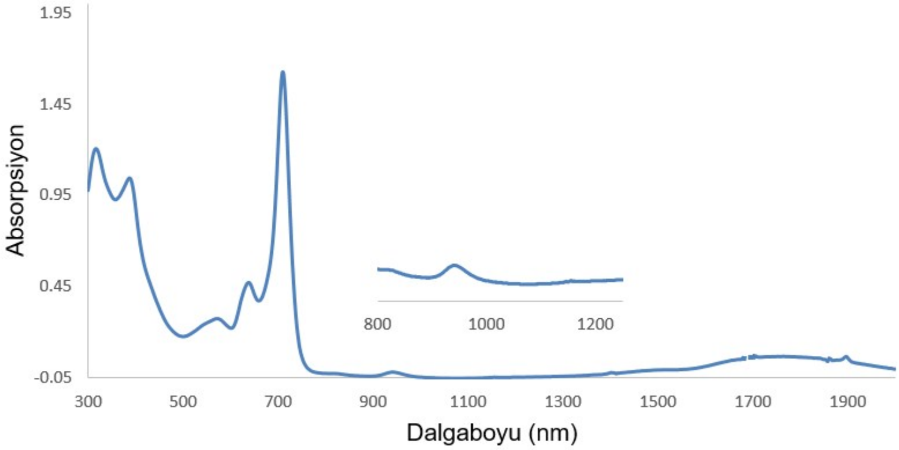

Figure S38 UV–vis and NIR spectra of **EuPc(Pox)[Pc’(AB_3OH)]** in neutral state in $CHCl_3$.

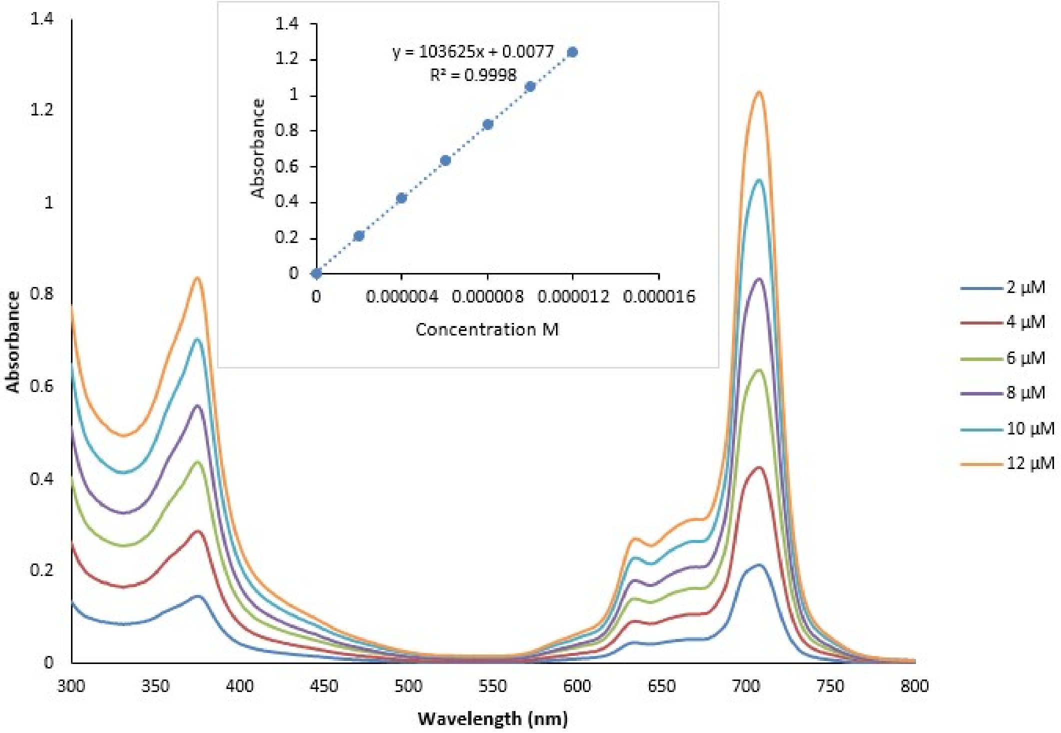

Figure S39 UV-Vis spectra of **LuPcPox(OAc)** at the different concentrations in DMSO.

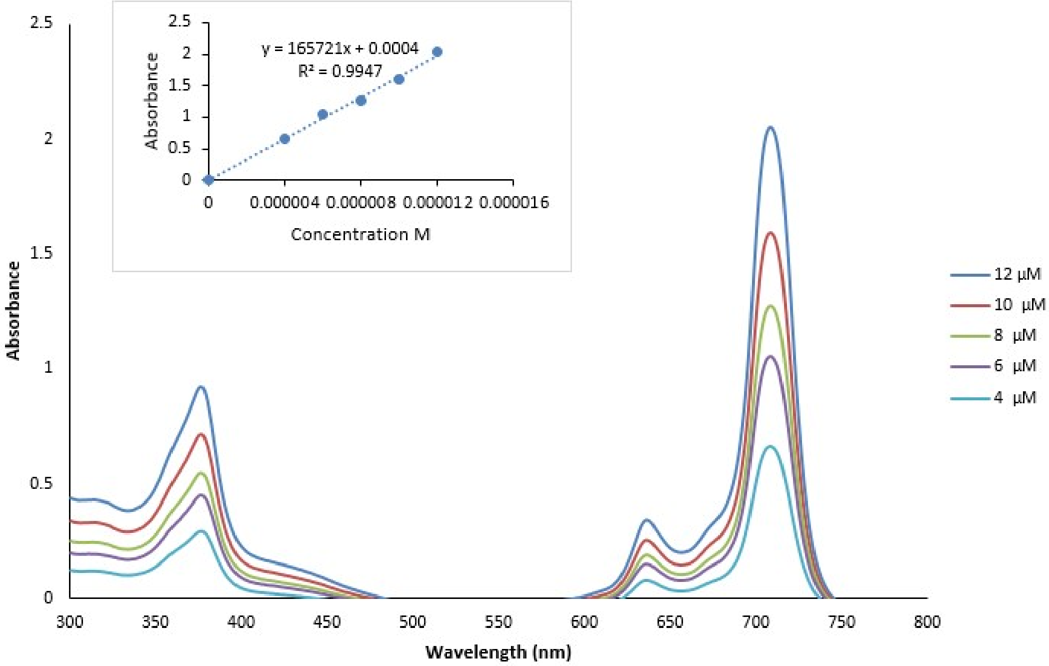

Figure S40 UV-Vis spectra of **EuPcPox(OAc)** at the different concentrations in DMSO.

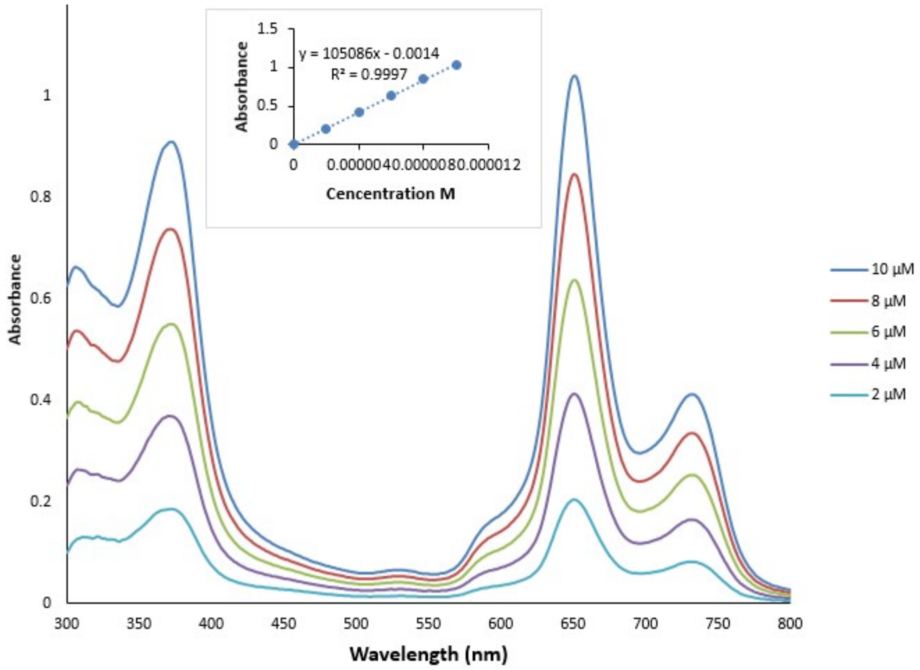

Figure S41 UV-Vis absorption spectra of **LuPc(Pox)[Pc’(AB_3SH)]** (reduced form in DMSO with NaBH$_4$ solutions of 2–10 µM concentration range. Insets: absorbance *vs*. concentration.

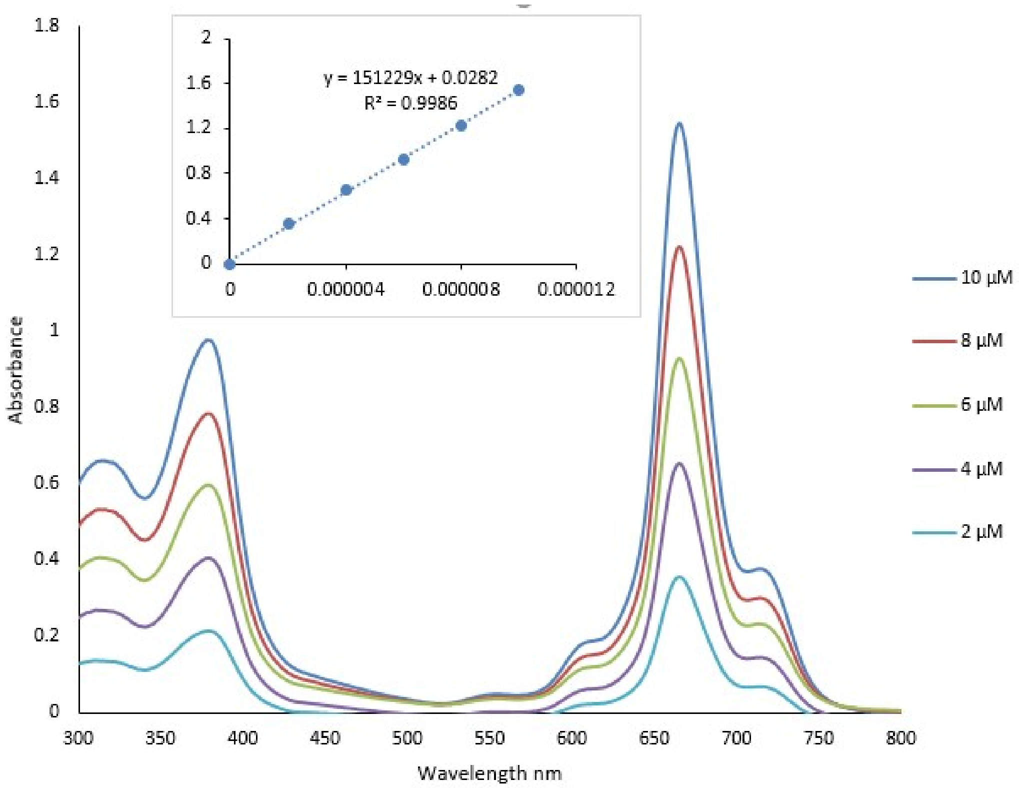

Figure S42 UV-Vis absorption spectra of **EuPc(Pox)[Pc’(AB_3SH)]** complex solutions in (reduced form in DMSO with NaBH$_4$ solutions of 2–10 µM concentration range. Insets: absorbance *vs*. concentration.

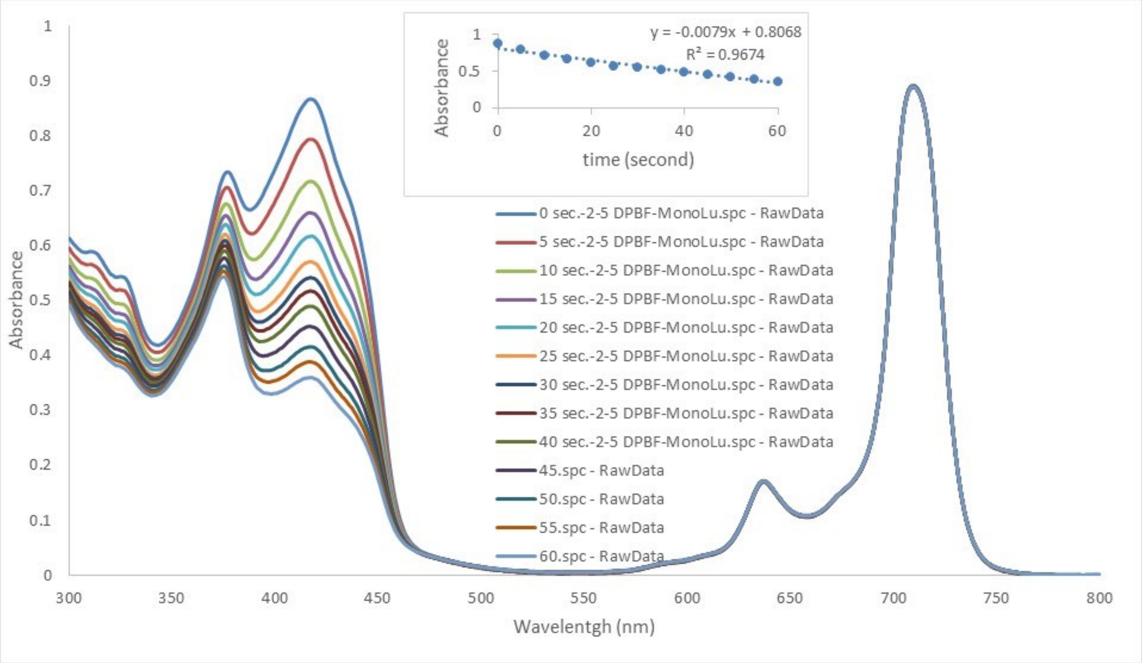

Figure S43 Determination of singlet oxygen quantum yield of **LuPcPox(OAc)** in DMSO. Inset: Plot of DPBF absorbance at 417 nm vs time.

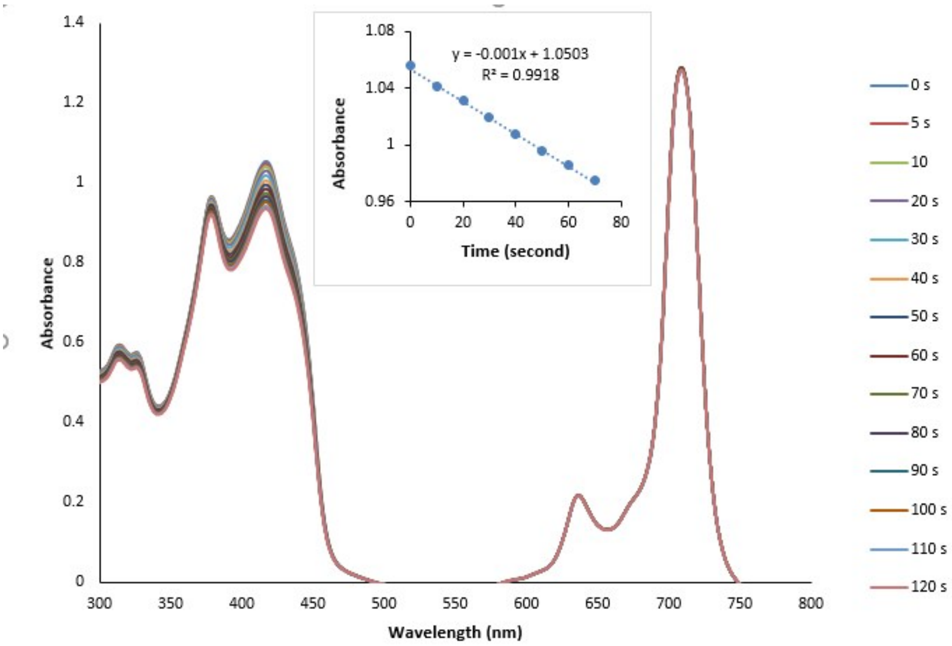

Figure S44 Determination of singlet oxygen quantum yield of **EuPcPox(OAc)** in DMSO. Inset: Plot of DPBF absorbance at 417 nm vs time.

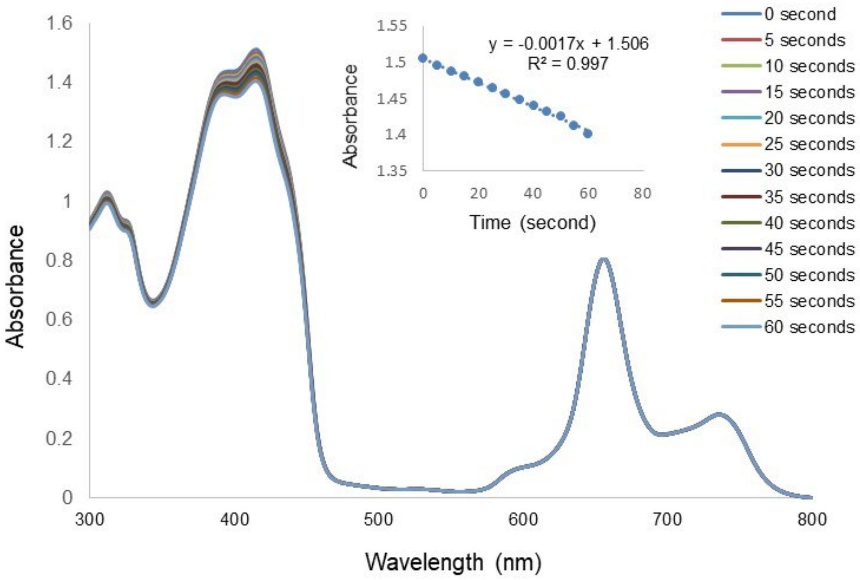

Figure S45 Determination of singlet oxygen quantum yield of **LuPc(Pox)[Pc'(AB$_3$SH)]** in DMSO. Inset: Plot of DPBF absorbance at 417 nm vs time.

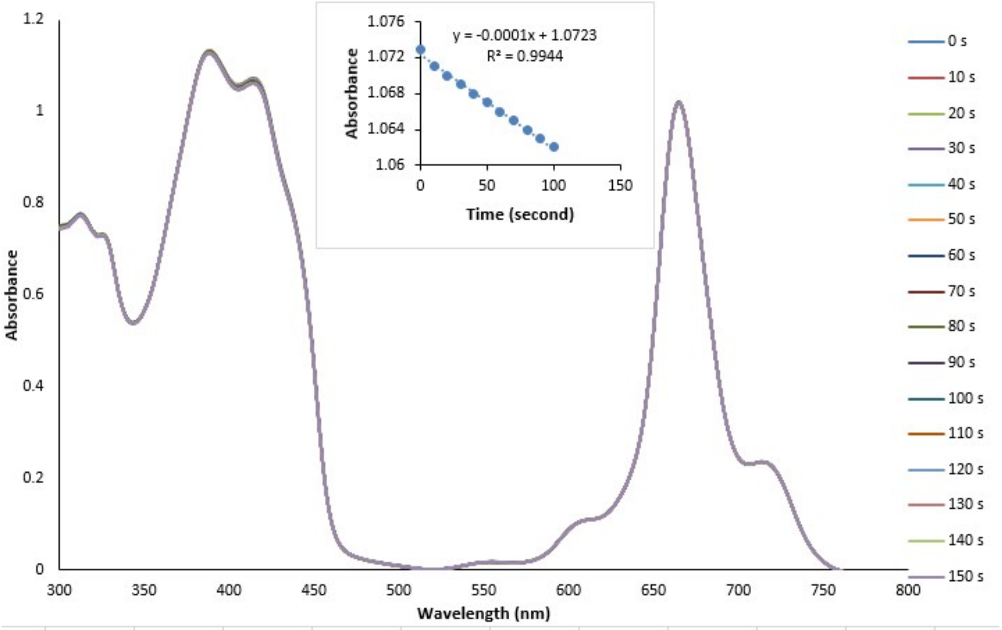

Figure S46 Determination of singlet oxygen quantum yield of **EuPc(Pox)[Pc'(AB$_3$SH)]** in DMSO. Inset: Plot of DPBF absorbance at 417 nm vs time.

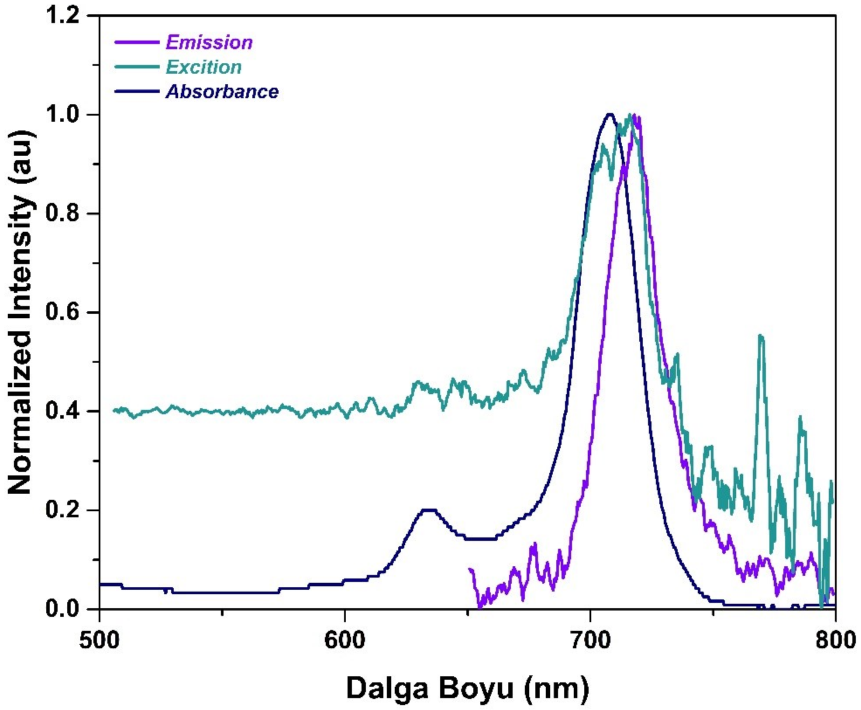

Figure S47 Electronic absorption, excitation and emission spectra of **LuPcPox(OAc)**

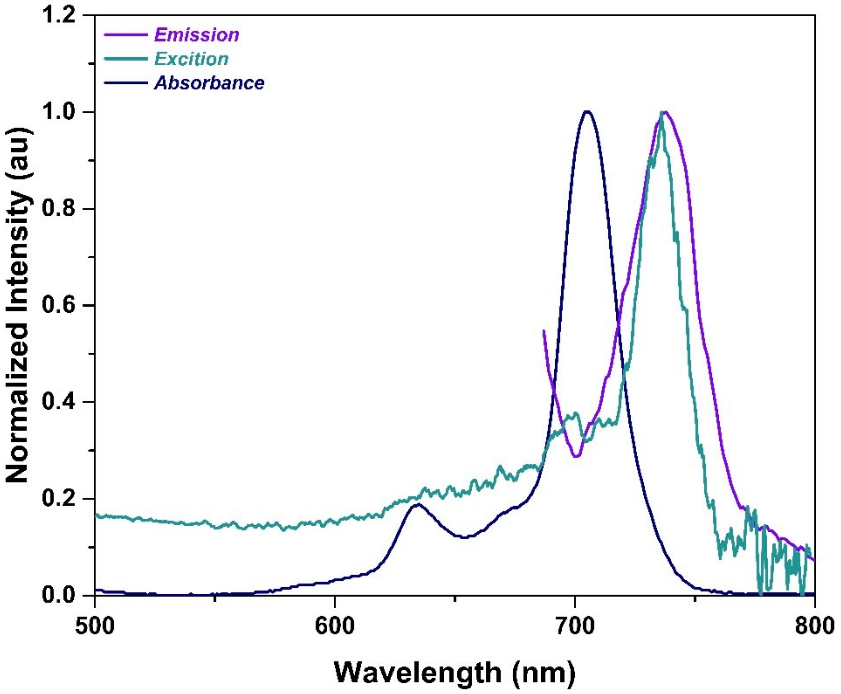

Figure S48 Electronic absorption, excitation and emission spectra of **EuPcPox(OAc)**

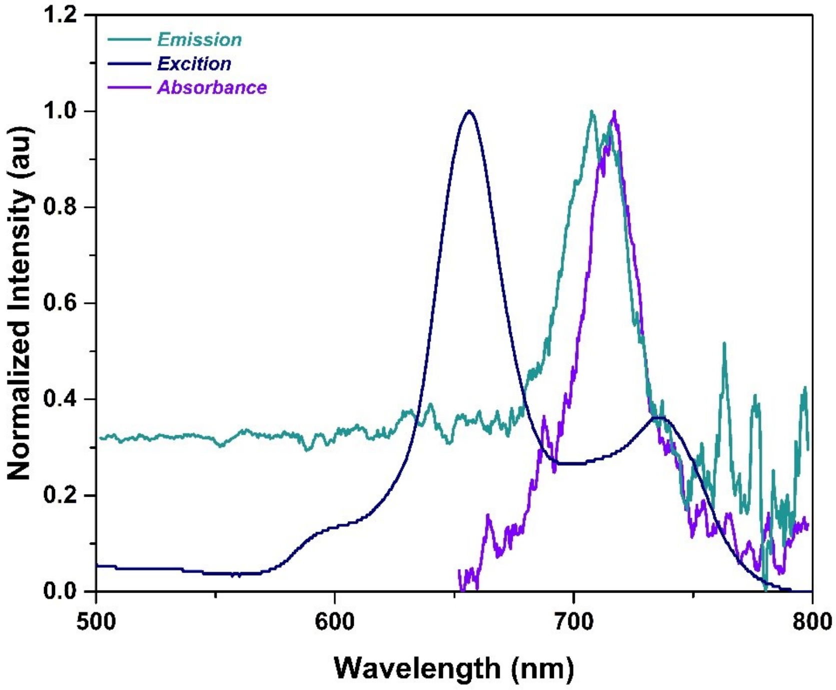

Figure S49 Electronic absorption, excitation and emission spectra of **LuPc(Pox)[Pc’(AB$_3$SH)]**

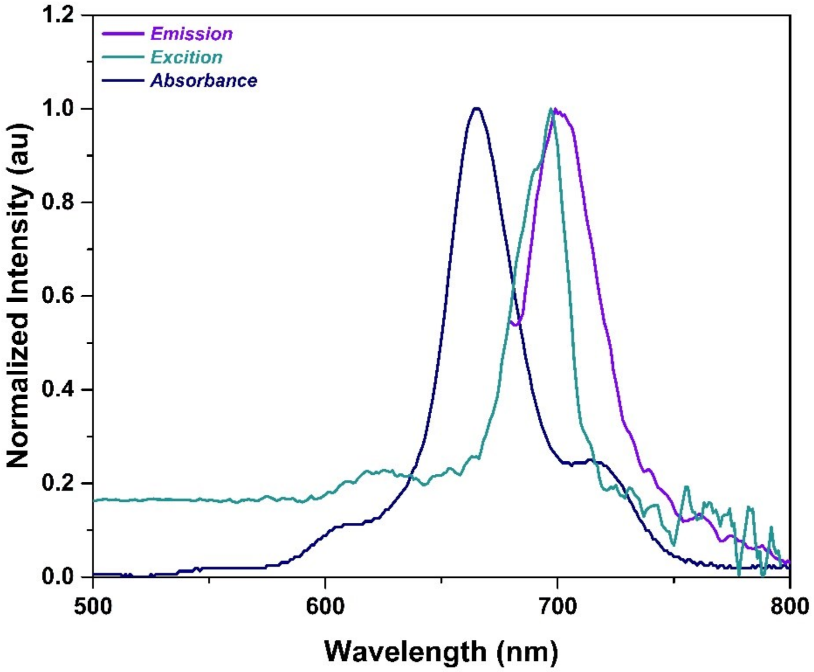

Figure S50 Electronic absorption, excitation and emission spectra of **EuPc(Pox)[Pc’(AB$_3$SH)]**

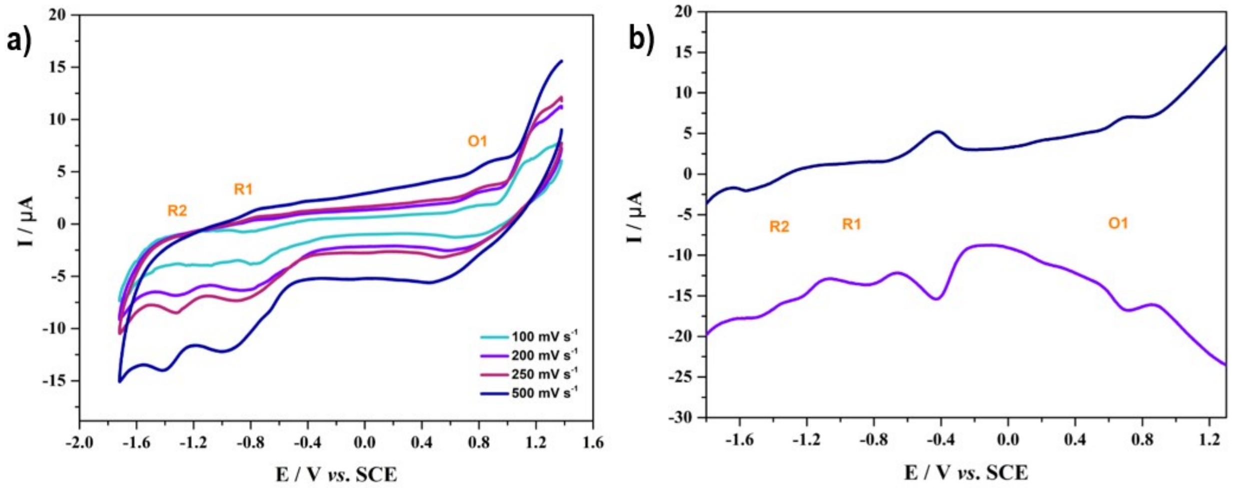

Figure 51: a) CVs of **EuPcPox(OAc)** at various scan rates on Pt in DCM/TBAP. b) SWV of **EuPcPox(OAc)**, SWV parameters: pulse size = 100 mV; Step Size: 5 mV; Frequency: 25 Hz.

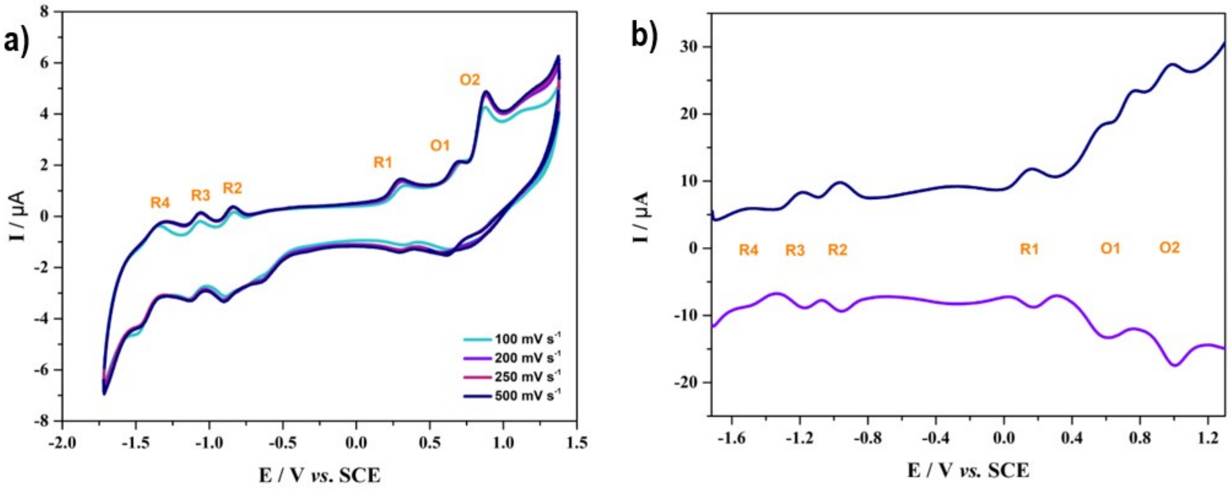

Figure 52: a) CVs of **EuPc(Pox)[Pc'(AB$_3$SH)]** at various scan rates on Pt in DCM/TBAP. b) SWV of **EuPc(Pox)[Pc'(AB$_3$SH)]**, SWV parameters: pulse size = 100 mV; Step Size: 5 mV; Frequency: 25 Hz.

5. Cell Viability

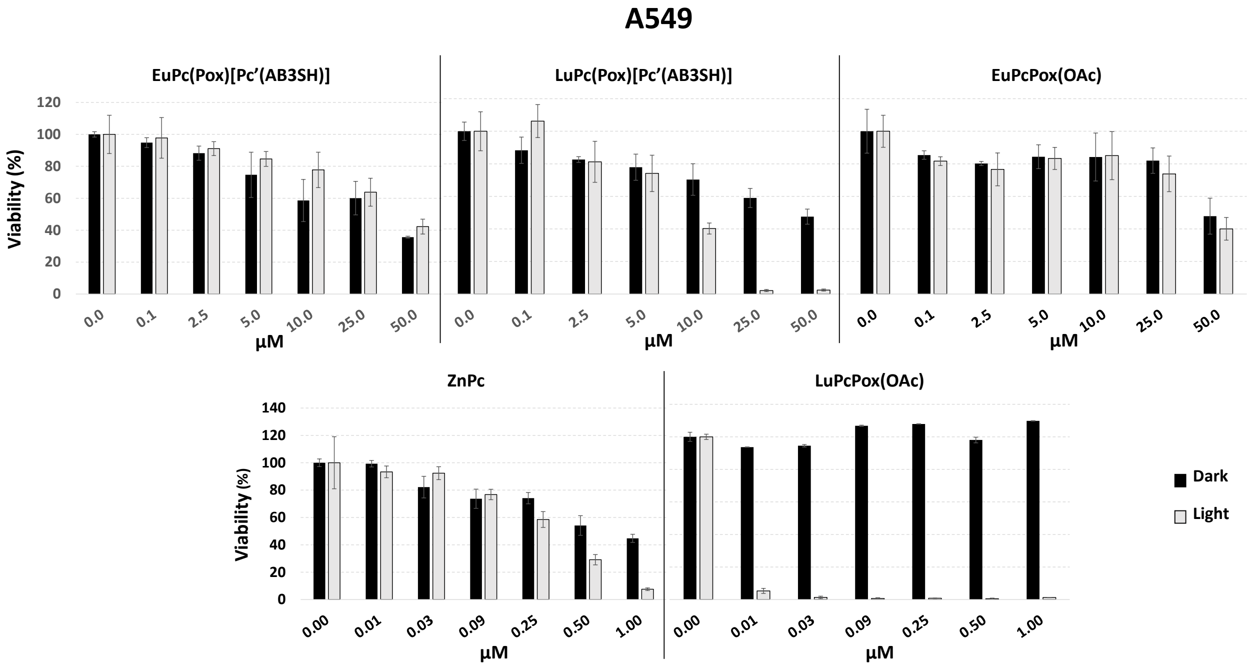

Figure S53 MTT results for 48h treatment of Pcs in A549 cells.

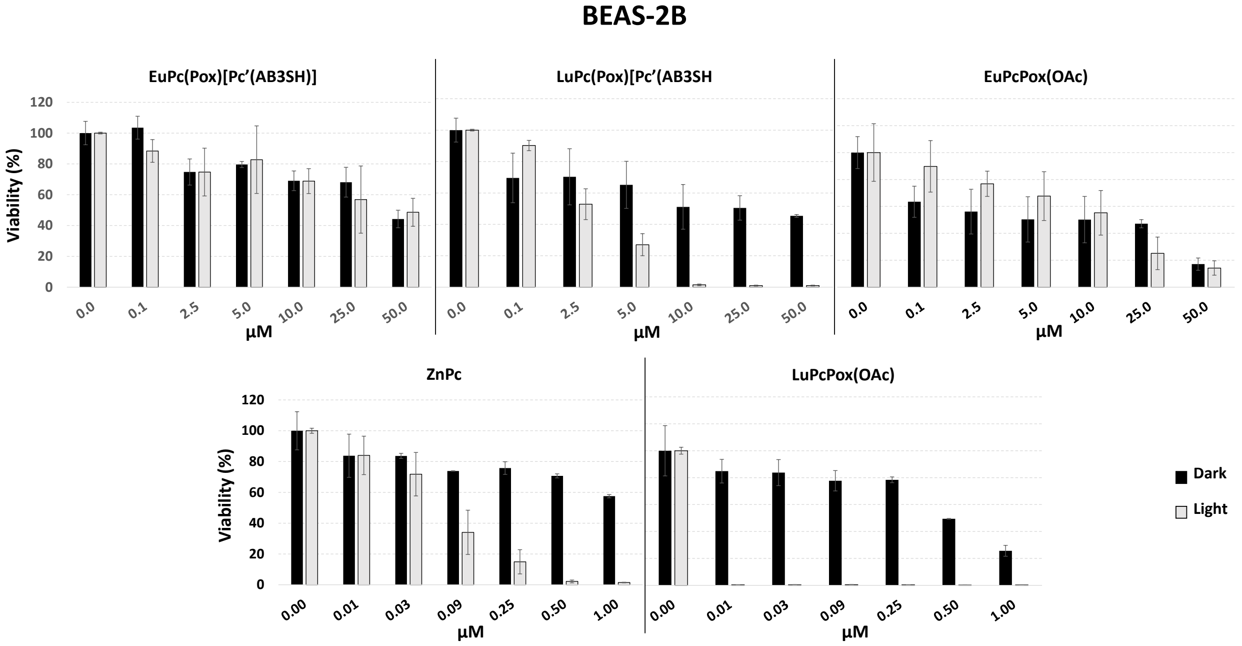

Figure S54 MTT results for 48h treatment of Pcs in BEAS-2B cells.

$$y = A1 + \frac{A2 - A1}{1 + 10^{(LOGx0 - x)p}}$$

A1: bottom asymptote

A2: top asymptote

LOGx0: center

P: hill slope

Figure S55 Dose-response curve fitting equation and parameters

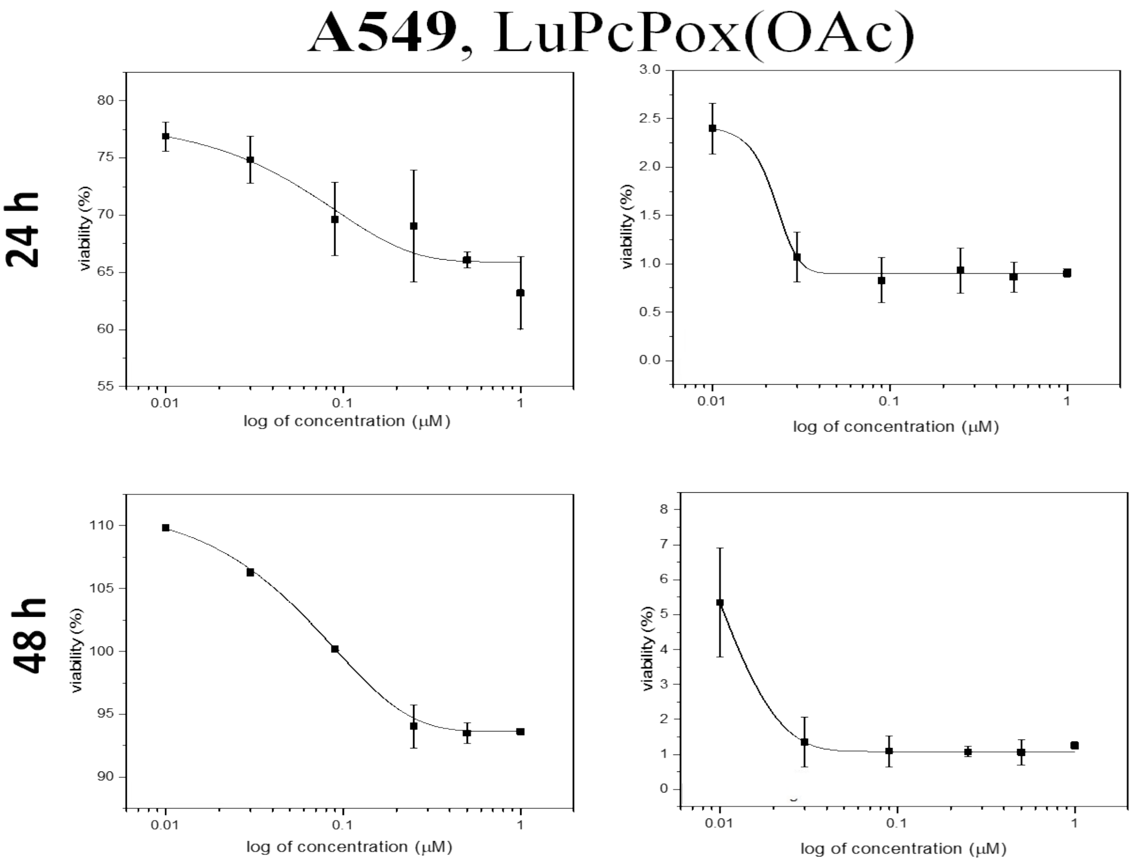

Figure S56 IC50 curves for LuPcPox(OAc) in A549 cells.

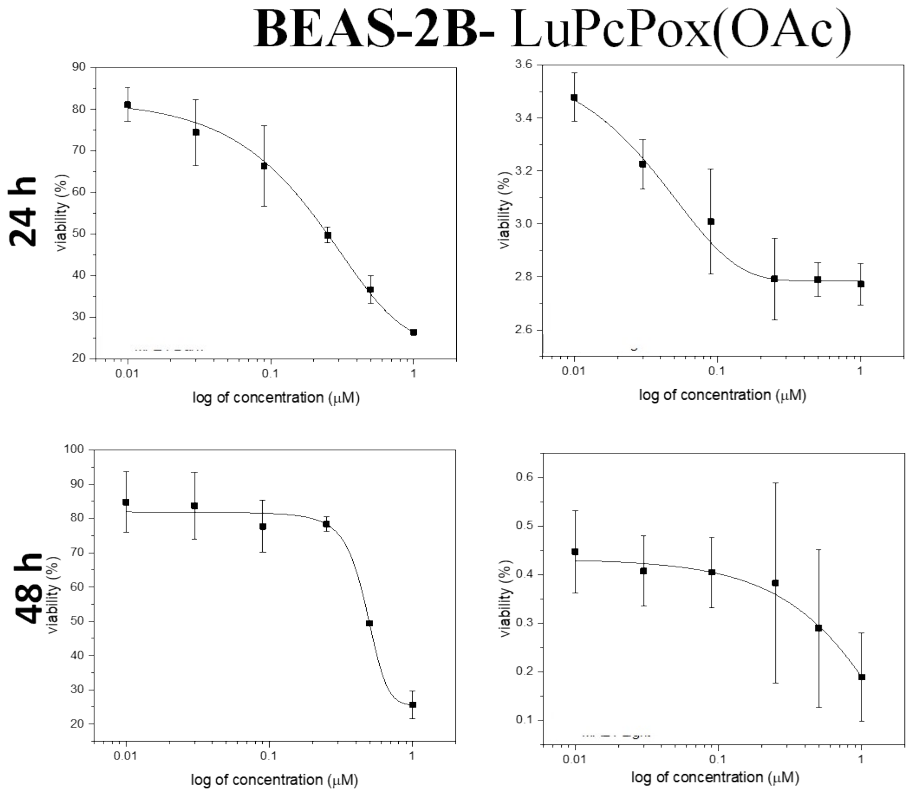

Figure S57 IC50 curves for LuPcPox(Oac) in BEAS-2B cells.

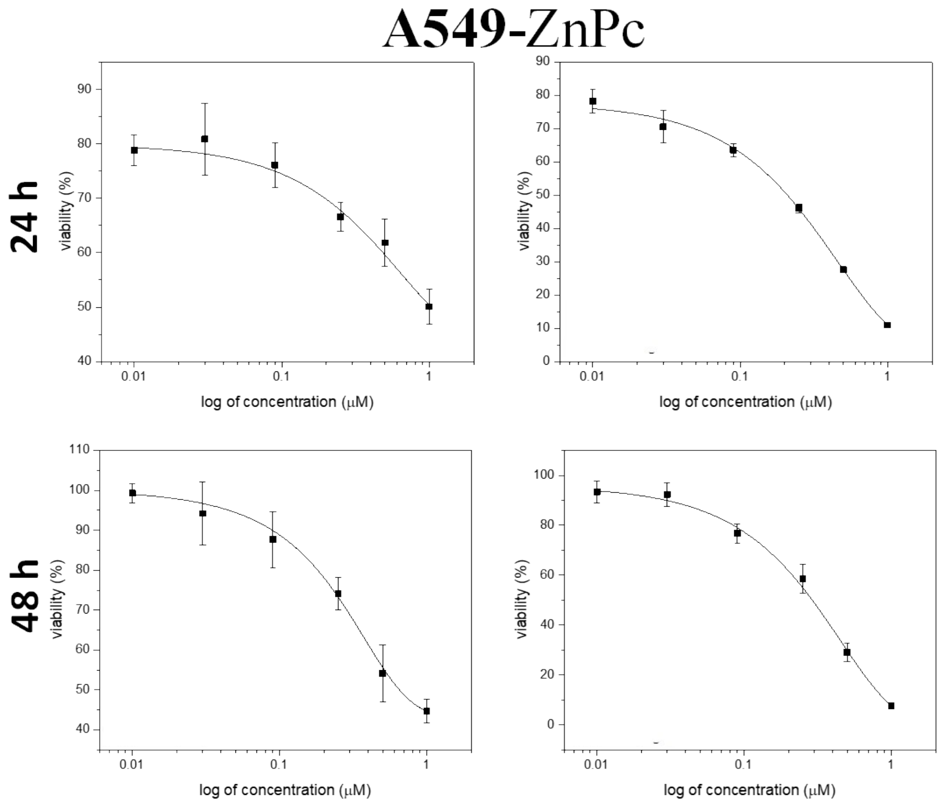

Figure S58 IC50 curves for ZnPc in A549 cells.

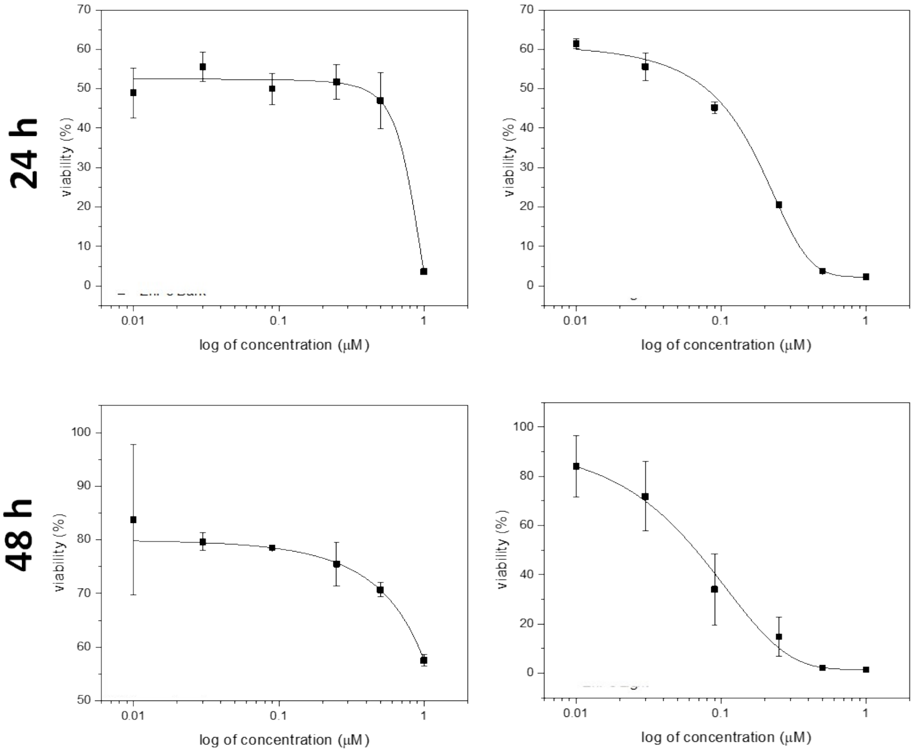

BEAS-2B-ZnPc

Figure S59 IC50 curves for ZnPc in BEAS-2B cells.

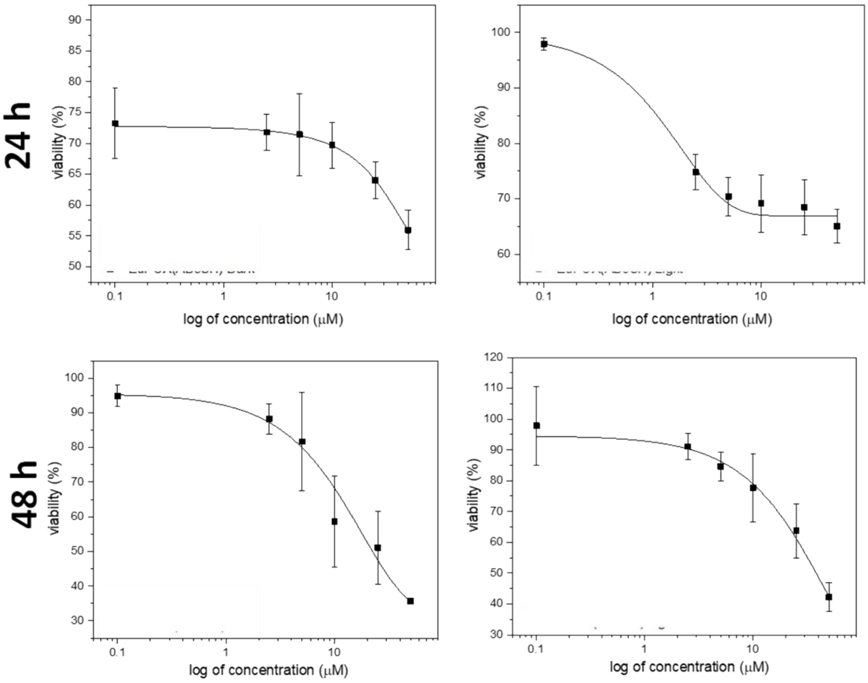

A549-EuPc(Pox)[Pc’(AB3SH)]

Figure S60 IC50 curves for EuPc(Pox)[Pc’(AB3SH)] in A549 cells.

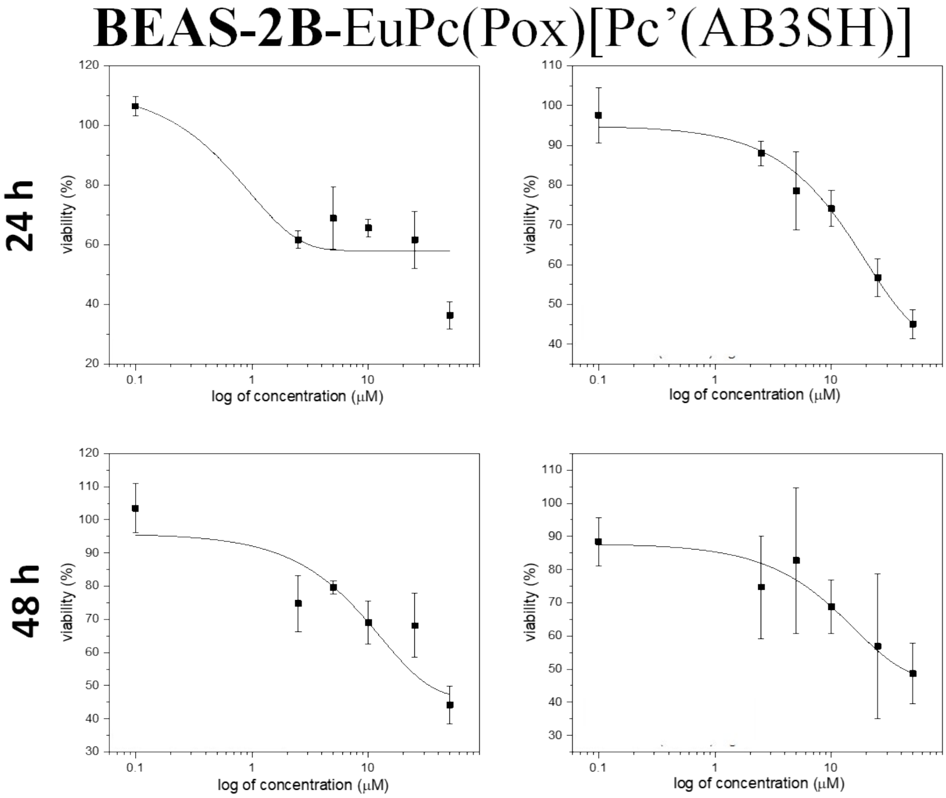

Figure S61 IC50 curves for EuPc(Pox)[Pc'(AB3SH)] in BEAS-2B cells.

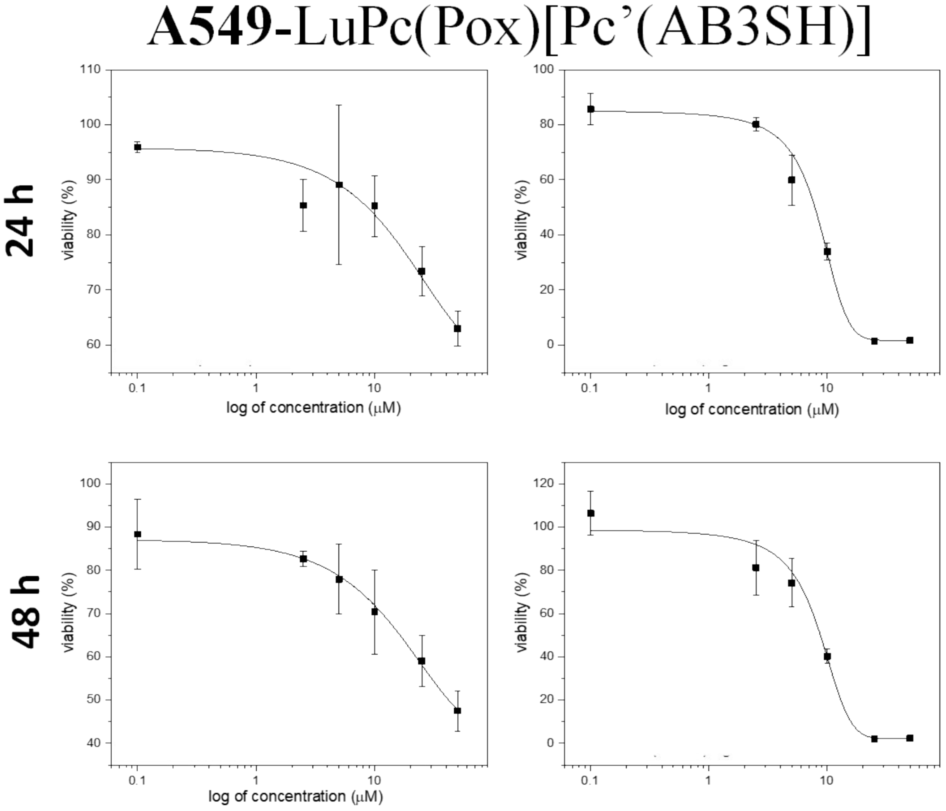

Figure S62 IC50 curves for LuPc(Pox)[Pc'(AB3SH)] in A549 cells.

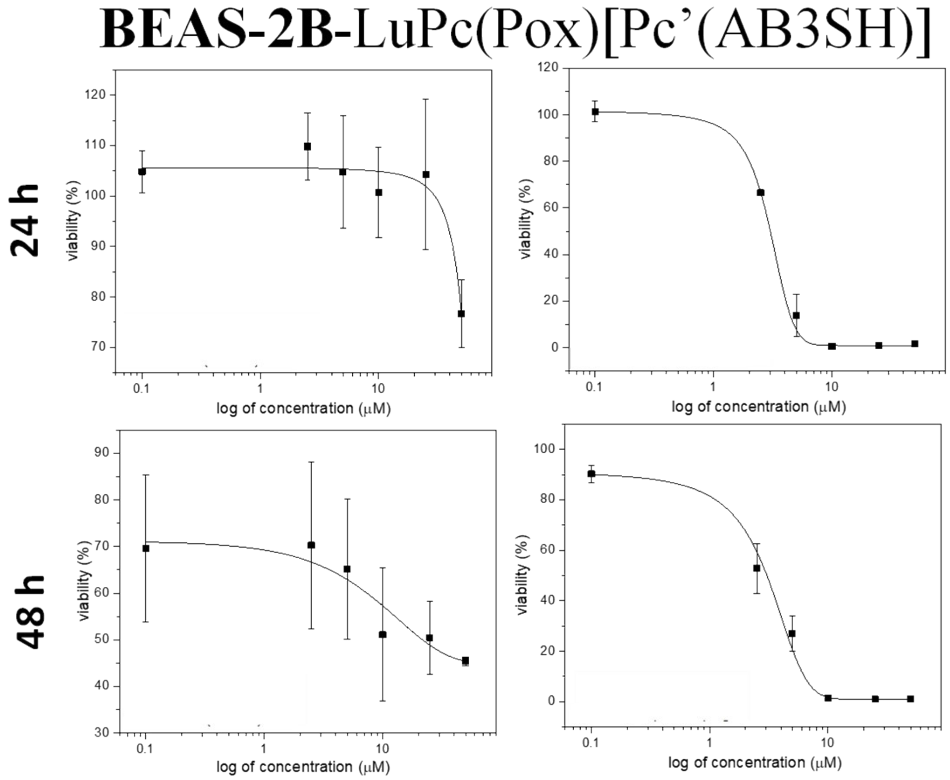

Figure S63 IC50 curves for LuPc(Pox)[Pc'(AB3SH)] in BEAS-2B cells.

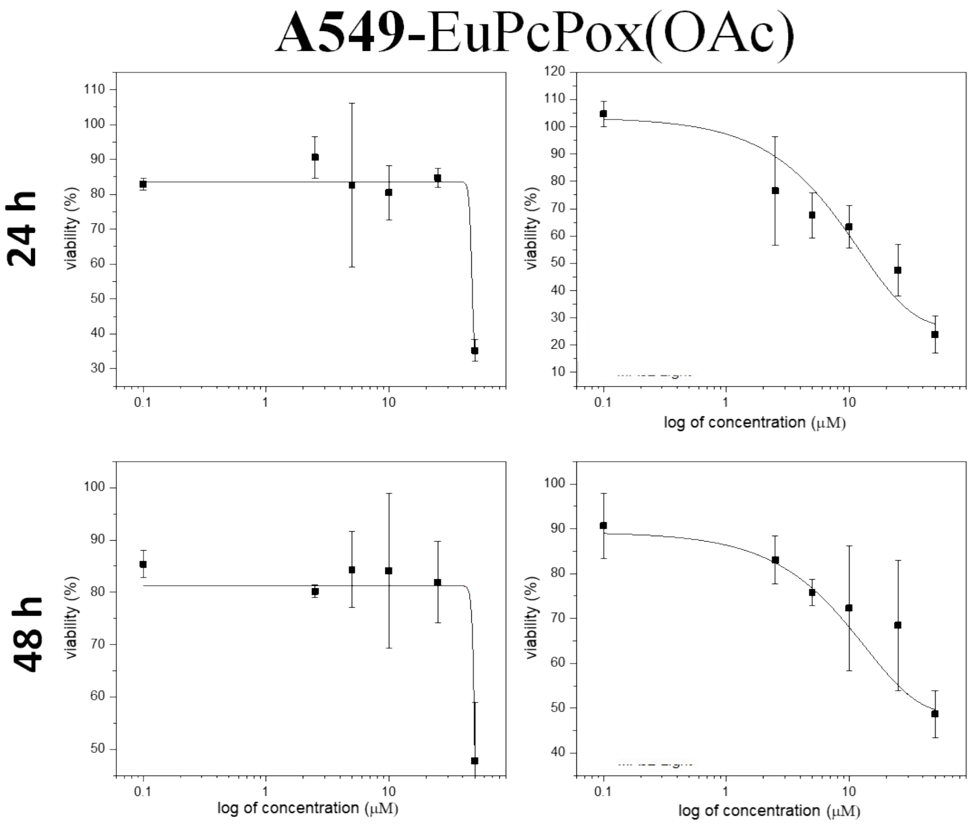

Figure S64 IC50 curves for EuPcPox(OAc) in A549 cells.

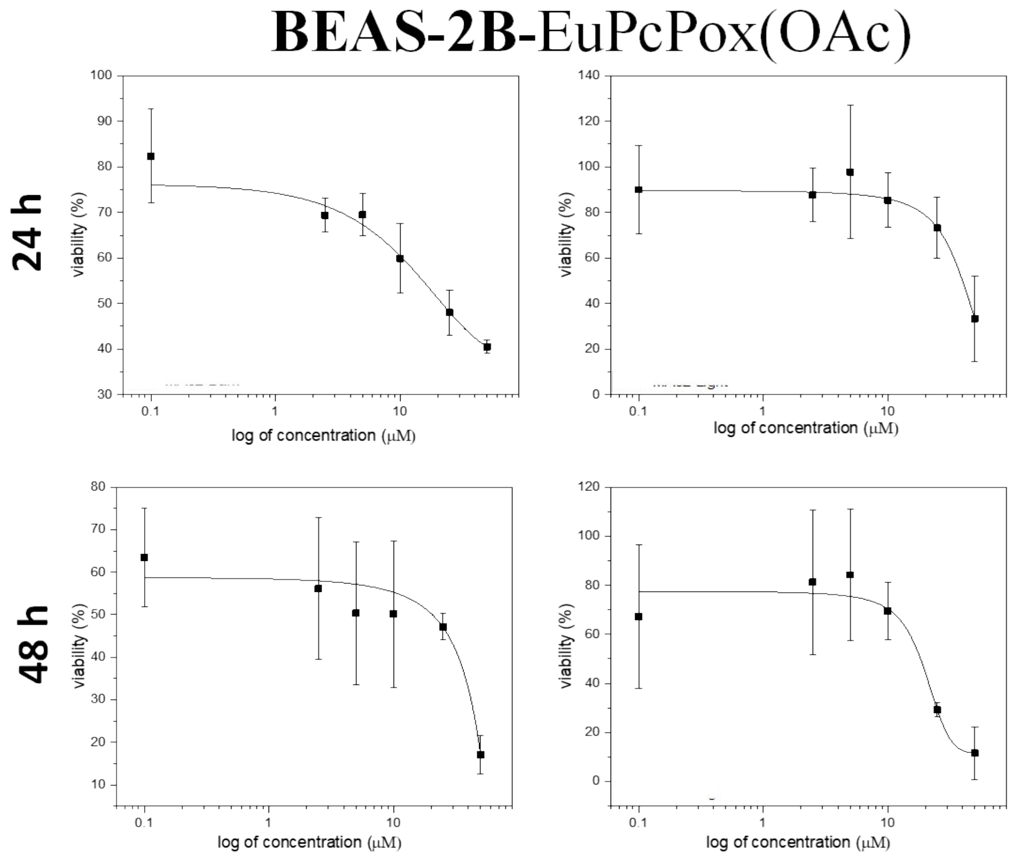

Figure S65 IC50 curves for EuPcPox(OAc) in BEAS-2B cells.

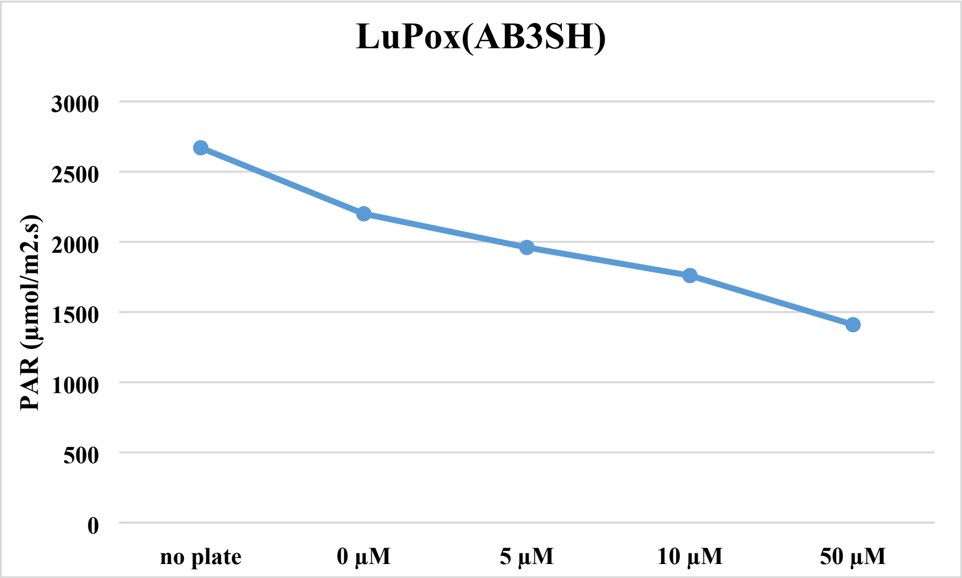

Figure S66 PAR measurements with increasing concentration of **LuPc(Pox)[Pc’(AB3SH)**

References

1. A. T. R. Williams, S. A. Winfield and J. N. Miller, *Analyst*, 1983, **108**, 1067-1071.
2. P. Jacques and A. M. Braun, *Helvetica Chimica Acta*, 1981, **64**, 1800-1806.
3. A. Ogunsipe and T. Nyokong, *Journal of Photochemistry and Photobiology A: Chemistry*, 2005, **173**, 211-220.
4. N. Kuznetsova, N. S. Gretsova, E. A. Kalmykova, E. Makarova, S. N. Dashkevich, V. Negrimovsky, O. Kaliya and E. Lukyanets, *Russian Journal of General Chemistry*, 2000, **70**, 133-140.
5. S. Z. Topal, Ü İşci, U. Kumru, D. Atilla, A. G. Gürek, C. Hirel, M. Durmuş, J. B. Tommasino , D. Luneau ,S. Berber, F. Dumoulin, V. Ahsen, *Dalton Trans.* 2014, **43**, 6897–6908
6. M. Thelakkat and H.-W. Schmidt, *Advanced Materials*, 1998, **10**, 219-223.
7. V. Novakova, B. Małachwiej, R. Šebl, M. Miletin and P. Zimcik, *Journal of Porphyrins and Phthalocyanines*, 2017, **21**, 302-310.
8. D. Woehrle, M. Eskes, K. Shigehara and A. Yamada, *Synthesis*, 1993, **1993**, 194-196.
9. A. G. Gürek, V. Ahsen, F. Heinemann and P. Zugenmaier, *Molecular Crystals and Liquid Crystals Science and Technology. Section A. Molecular Crystals and Liquid Crystals*, 2000, **338**, 75-97.